Utrecht University

Institute for Theoretical Physics

Master's Thesis

The probability of primordial black hole formation

Author:
Rik van der Stelt, BSc

Supervisor:
Dr. Tomislav Prokopec

July 15, 2019

Universiteit Utrecht

Abstract

Primordial black holes might make up dark matter, and their abundance is a sensitive probe of the amount of small-scale fluctuations in the early universe and of the theory of inflation that sourced them. In this thesis, we present a calculation of their formation probability in the radiation era directly from the density matrix of any inflationary state seeding the density perturbations for their production, using the Wigner function to define probability distributions of the relevant quantum fields. For Gaussian states and a Gaussian distribution of the overdensities, this yields a well-defined prescription to link the local power spectrum to the nonlocal probability of a region to collapse. We find corrections to previously found results due to nontrivial momentum correlators, and suggest that these might also influence the formation criteria. Extensions of this method to study non-Gaussianity and shape-dependence of the formation criteria are within reach.

Contents

Definitions and conventions

In this thesis, we use the natural units $\hbar = c = 1$. We will also use both Newtons gravitational constant G and the reduced Planck mass $M_p^2 = (8\pi G)^{-1}$, which we will occasionally set to one.
Our Fourier transform convention is:

$$\tilde{f}(k) = \int_{-\infty}^{\infty} dx e^{-ikx} f(x).$$

Our metric signature is $(-,+,+,+)$.

We denote four-vectors x_μ with Greek indices, and three-vectors x_i with Latin indices.

Throughout, we use lower-case for comoving coordinates and momenta, and capital letters for physical coordinates and momenta. We will also often denote the norm of a 3-vector $\vec{k}$ by k.

Introduction

The nature of dark matter is one of the greatest and most enduring mysteries in physics, and perhaps in all of science. After over 80 years of searching, we still cannot claim to have any knowledge about what it consists of, apart from that it barely interacts with regular matter, is nonrelativistic and nonbaryonic and is found in halos around galaxies. [1] There is a wide variety of theories on what it could be though, from unknown subatomic particles, to clouds of gas, to even a change in the laws of gravity itself. One particularly interesting candidate for dark matter is the primordial black hole (PBH) [2]. These are black holes that form right after the big bang, in the first second of the universe, from the collapse of large overdensities in the extremely dense primordial plasma [3, 4]. They can form with any mass and size, from subatomic to supermassive, depending on the size of the overdense region. This makes them not only interesting as dark matter candidates, but also as the source of the absurdly massive black holes in the centres of galaxies or the black hole binaries measured by LIGO.

The amount of PBHs that form is determined by how many sufficiently large overdensities are caused by metric and matter fluctuations in the early universe. To calculate this, we need to both know when an overdensity is sufficiently large and what the distribution of overdensities is like. The first question already proves to be a very tough one, with multiple criteria defined over the years yielding different results. We will follow the results from Musco [5], who posed a criteria in terms of the compaction function for a spherical volume, which is defined as:

$$\mathcal{C}(r,t) = \frac{2G\delta M(r,t)}{2a(t)r},$$

where $\delta M(r,t)$ is the excess mass in the volume and a the scale factor. To determine the distribution of $\mathcal{C}$, we need to relate it to the primordial curvature perturbations. This is possible because the mass excess can be related to the density perturbation, which is sourced by the curvature perturbations via a relativistic Poisson equation. Inflation then tells us what the fluctuations are like. In particular, for the commonly accepted slow roll (SR) scalar field inflation, these perturbations are way too small to form any PBHs, since it predicts that the spectrum is nearly scale invariant and

the perturbations at large scales measured in the cosmic microwave background (CMB) and large scale structure (LSS) are really small. Therefore, to form any significant amount of PBHs a theory beyond SR single field inflation is needed. We will not study these theories specifically, but take a general power spectrum with enhancement on small scales as our input. The main purpose of this thesis is then to calculate the PBH abundance for any such theory.

To calculate the probability of a certain region collapsing to a PBH, we need to calculate the probability of the field $\mathcal{C}(r,t)$ to have a given value. This is most naturally done in the framework of the Wigner function, where we can properly define a probability distribution for the quantum field in the Gaussian state that describes inflation. Using this, we can calculate a probability distribution for $\mathcal{C}$ from first principles with only the density matrix or the Gaussian correlators of the inflationary theory as input. It turns out however, that not only the curvature power spectrum plays a role, but also the momentum correlators. These are not usually taken into account in numerical studies, and are often not very well known in theories of beyond slow roll inflation, so one of the main messages of this thesis is that more attention should be paid to them, both in numerical simulations of PBH formation and analytical studies of beyond slow roll inflation.

Using this framework, and integrating over the momentum correlators, we then calculate the probability of PBH formation and find a formula that both extends results found earlier and specifies how the power spectrum in Fourier space should be related to the mass scale of the PBH that forms. It is found that the amount of PBHs that form is very dependent on the amplitude of the enhancement on small scales, and hence that any inflationary model producing enough PBHs to be dark matter must be extremely fine-tuned, or have some mechanism stabilising it at the value needed to produce the right amount.

In this thesis therefore, we find a general framework with which the amount of PBHs that forms can be calculated from any Gaussian theory of inflation. This formalism also allows us to take into account how the evolution of cosmological perturbations affects the formation of primordial black holes. Therefore, this can rule out certain theories that produce too much PBHs, since they can at most be all of the dark matter in the universe. Also, if PBHs were ever to be detected, this would rule out theories that produce too little of them. In particular, the standard slow roll scalar field inflation produces no primordial black holes, so any discovery would mean that this cannot be the full picture. Black holes formed from stellar collapse have a minimal mass on the order of a solar mass [6], so any measurement of a lighter black hole would mean a discovery of a PBH, since no other formation mechanisms are known. Similarly, if studies of galactic dynamics would show that the supermassive and intermediate mass black holes need to have primordial origins, this would mean

that inflation cannot be described by slow roll alone. The amount of PBHs in our universe is intimately linked with the specifics of inflation, and might be the only way to probe its small scale behaviour.
In chapter 1 of this thesis we review how the dark matter mystery became apparent in the last 80 years, the numerous evidence for its existence and how PBHs can solve this mystery. Along the way, we will develop some basic results in cosmology for later use, and describe what the criteria are for the formation of PBHs. In chapter 2 we introduce inflation and the framework of cosmological perturbation theory with which we can describe the fluctuations in the early universe that source the overdensities that collapse to form the PBHs. In chapter 3, we introduce the Wigner function formalism with which we will calculate the probability density for $\mathcal{C}$. In chapter 4 we present our results for the calculation of the probability of PBH formation in the early universe for a number of theories of inflation. Chapter 5 is reserved for a discussion of our main results and in appendices we present some important technical details of our calculations.

Chapter 1

The dark universe

1.1 Evidence for dark matter

For over eighty years, physicists have been puzzled by the missing matter in the universe. In this section, we will briefly mention the main pieces of evidence from different observations that have guided the search, as well as describe some of the most studied candidates and how they fare under experimental scrutiny. We will mostly follow [1].

1.1.1 First hints

The first known mention of "dark matter", perhaps somewhat suprisingly, predates its first observation by over 30 years. Astronomers in the late nineteenth and early twentieth century were well aware that a significant portion of the mass in our galaxy could be in objects that do not emit any light. However by studying the velocity dispersion of the stars in our neighbourhood, it was concluded by astronomers such as Ernst Öpik in Estonia and Jacobus Kapteyn in Groningen that the amount of "dark matter" in the universe was small [1].

The first suggestion that this might not be the complete picture came when astronomers started looking at structures outside our galaxy. In the 1930s, Fritz Zwicky was studying the motion of galaxies in a number of clusters, among which was the Coma cluster when he noticed that the relative velocities of the galaxies were much bigger than expected [7]. By the virial theorem, these velocities are related to the total mass of the system, which could also be estimated from the luminosity of the galaxies. The mass he inferred from the velocities was 400 times greater than what was expected from the visual sources, leading him to conclude that most of the matter in the cluster was dark. We know now that this factor of 400 is mainly due to the fact that he used a value for the Hubble constant which was off by an order of magnitude, but taking this into account still a large mismatch remains.

At the time, this discovery was not seen as a big breakthrough, but rather as a sign of how little was known about galaxies, which were only discovered barely twenty years earlier. Zwicky himself thought this dark matter consisted of "nebulae in the form of cool and cold stars, macroscopic and microscopic solid bodies, and gases"[8]. Another popular explanation was that the clusters were not actually virialised but rapidly expanding, and that application of the virial theorem was therefore invalid. In the following years however, these theories started to lose ground. Surveys of the amount of gas in galaxies found way too little to explain the large velocities, and it was also realised that the galaxies could not be rapidly expanding, since they would then have already evaporated a long time ago. Astrophysics was left with a mystery, which would only get more puzzling when the next experimental evidence came in.

1.1.2 Rotation curves

The rotation of stars around the centres of galaxies had already been studied since the 1930s. However, it was only in the early 1970s that measurements on the rotation velocity could be reliably made far away from the centre of galaxies. This could then be compared with optical and 21 cm data which determined the distribution of stars and gas inside galaxies, which found that most of the visible mass of a galaxy is near its core, and that the density falls off exponentially at large radii. From this it would be expected that the rotation velocity also falls off at larger radii, as is the case for orbits around a point mass. This turned out not to be the case: the rotation curves remain constant up to the edges of galaxies. The most natural explanation was that there is not just visible mass in galaxies, but also invisible mass, dark matter, in a halo surrounding the galaxy. In figure 1.1, some of the data from 1972 showing this effect can be seen, but it must be noted that there were many different groups doing these experiments, all finding the flattening of the curves. At the end of the decade these results, and with them the fact that most of the mass in galaxies was dark, had become well-accepted.

1.1.3 Evidence from cosmology

In the end, the most convincing evidence for the existence of dark matter arguably came from cosmology. In the 1970s and 80s, accurate calculations and experiments on the early universe made it clear that only a small fraction of the matter in the universe could consist of baryons. In this section, we will broadly sketch the basics of cosmology and explain how these measurements could be made.

The starting point of cosmology is the fact that the universe is homogeneous and isotropic on large scales. The isotropy has been observationally confirmed by the large

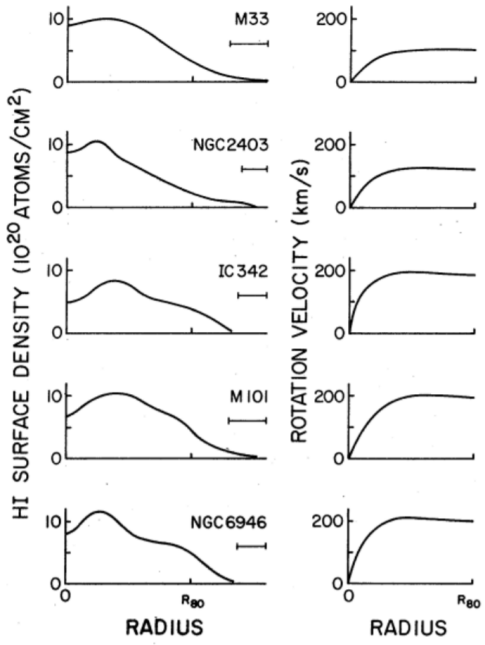

Figure 1.1: Rotation curves for a number of galaxies as found by Rogstad and collaborators in 1972 [9]. In the left column the density of gas is plotted, and on the right the rotation velocity, both as a function of the distance from the centre. The flattening can clearly be seen.

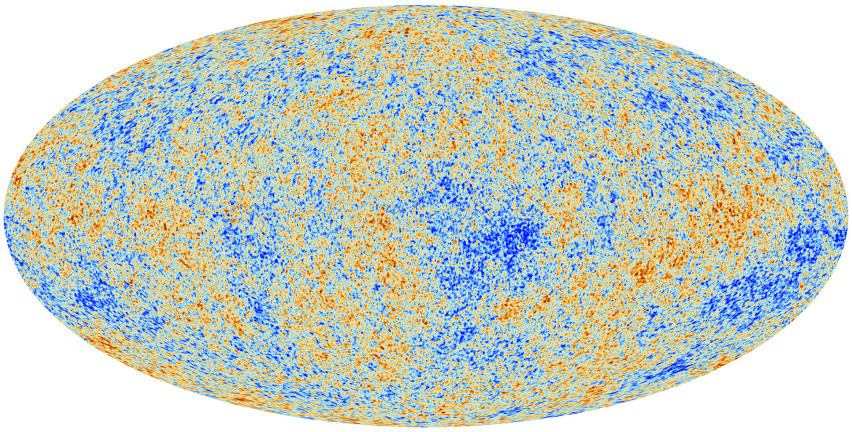

Figure 1.2: The temperature fluctuations in the cosmic microwave background. The temperature difference between patches is of the order of $10^{-5}T_0$, with $T_0 \approx 2.7K$. Image: ESA and the Planck Collaboration.

scale structure of galaxies and especially by the isotropy of the cosmic microwave background (CMB). The temperature fluctuations seen in figure 1.2 are only on the order of 10^{-5}, so this assumption seems to be pretty good. This does not directly imply homogeneity, but an isotropic but inhomogeneous universe in which we are at the centre of concentric homogeneous shells seems very unrealistic and contrived.

It has been known for a while that the only homogeneous and isotropic metric with which the universe can be described is the Friedmann-Robertson-Lemaitre-Walker (FLRW)metric, given by:[10]

$$ds^2 = -dt^2 + a^2(t)(\frac{\mathrm{d}r^2}{1-\kappa r^2} + r^2\mathrm{d}\Omega^2), \tag{1.1.1}$$

where $a(t)$ is the scale factor, $\mathrm{d}\Omega^2 is$and κ is a parameter that determines the global curvature and hence geometry of the universe: it is flat for $\kappa = 0$, positively curved and spherical for $\kappa > 0$ and negatively curved and hyperboloidal for $\kappa < 0$. The evolution of the scale factor is determined by the Einstein equations:

$$R_{\mu\nu} - \frac{1}{2}Rg_{\mu\nu} = \frac{1}{M_p^2}T_{\mu\nu}, \tag{1.1.2}$$

where $R_{\mu\nu}$ is the Ricci tensor, R the Ricci scalar and $M_p = (8\pi G)^{-1}$ the reduced Planck mass. The background of all matter sources of cosmological relevance can be described by a perfect fluid with pressure p and density ρ, such that we have the following stress-energy tensor:

$$T_\mu^\nu = \mathrm{diag}(-\rho, p, p, p). \tag{1.1.3}$$

The equation of state of the fluid is described by the parameter $\omega \equiv \frac{p}{\rho}$, which plays an important role in the evolution of the universe as we shall see. We also introduce another very important quantity here: the Hubble parameter:

$$H(t) \equiv \frac{\dot{a}(t)}{a(t)}. \tag{1.1.4}$$

This roughly describes how fast the expansion of the universe is happening, and gives the natural length scale of the problem, namely the Hubble length H^{-1} which will play a very important role in inflation. In terms of this, the Einstein equations then become:

$$H^2 = \frac{\rho}{3M_p^2} - \frac{\kappa}{a^2} \tag{1.1.5}$$

and

$$\dot{H} + H^2 = \frac{\ddot{a}}{a} = -\frac{1}{6M_p^2}(\rho + 3p), \tag{1.1.6}$$

which are called the first and second Friedmann equation. From the second equation we see the importance of the value of ω. If $\omega > -\frac{1}{3}$, $\ddot{a} < 0$ and the expansion of the universe slows down as time goes on, but if $\omega < -\frac{1}{3}$, the expansion accelerates.

At early times, the universe was extremely hot and dense, and therefore most of the particles were relativistic: the total energy came mainly from their kinetic energy. This is called the radiation dominated era. As the universe cooled down, the mass of the particles became the dominant source of energy and the universe entered the matter dominated era, in which most of the matter is nonrelativistic. In this case, we have $\omega = 0$, but for the fluid of relativistic particles in the radiation era we have $\omega = \frac{1}{3}$. The dark energy that dominates our universe has $\omega = -1$, but we will not be concerned with it further in this thesis, as it is negligible during the formation of PBHs.
It is also useful to transform the metric to conformal time $d\tau = \frac{dt}{a}$, such that it becomes the conformal Minkowski metric with a scale factor in front:

$$ds^2 = a^2(\tau)(-d\tau^2 + d\vec{x}^2), \tag{1.1.7}$$

for which an equivalent to the Friedmann equations can also be derived.
By integrating these equations, we find the evolution of a and ρ. The results for this are shown table 1.1, for both regular and conformal time.
One argument for dark matter came from experimental studies of the first Friedmann equation 1.1.5, measuring both H and ρ. A significant part of the cosmological community in the 1980s and 90s believed that the total density of the universe should be equal to the critical density $\rho_c = 3M_p^2H^2$, or, in other words, that the curvature κ should be 0. This flatness of the universe was also predicted by the newly postulated theory of inflation. Therefore, when measurements of visible matter

	w	$\rho(a)$	$a(t)$	$a(\tau)$
MD	0	a^{-3}	$t^{2/3}$	τ^2
RD	$\frac{1}{3}$	a^{-4}	$t^{1/2}$	τ
Λ	-1	a^0	e^{Ht}	$-\tau^{-1}$

Table 1.1: Evolution of various parameters as a function of both conformal and physical time for a universe dominated by matter (MD), radiation (RD) or a vacuum energy (Λ).

found a density much smaller than the critical density, it was proposed that dark matter could explain this discrepancy. Dark matter only turned out not to be enough however, and it was only when dark energy was discovered that it was found that the universe is flat after all. In fact, current CMB experiments show that κ is negligible to very high precision[11], and something that was at first a problem for inflation now is one of its strongest predictions.

The first clear evidence from cosmology that dark matter had to exist came from calculations on nucleosynthesis: the formation of the first atomic nuclei in the early radiation era around three minutes after the big bang. When the nuclear reactions causing this formation were carefully studied, it was found that the relative abundance of the different nuclei produced in this process like H-1, deuterium, He-3 and He-4 was strongly correlated with the total baryon density in the universe. By comparing the calculations with the observed deuterium abundance in the universe, it was already shown in 1972 that only 10% of the critical density could consist of baryons [12], and the constraints only got stronger as time went on, proving that baryons only make up a tiny fraction of the universe. The current constraint on baryon density is about $\Omega_b \simeq 0.05$ [11].

The second piece of evidence came from the temperature fluctuations in the CMB. Even though it is very homogeneous, there are still tiny temperature fluctuations. There are peaks and troughs in the power spectrum of these fluctuations, coming from acoustic density waves in the plasma of the early universe. The amplitude of these peaks turns out to be directly related to the total baryon density in the universe and again, measurements of the height of this peak confirmed that most of the energy in the universe could not be in baryonic matter.
In other words: dark matter could not just consist of dark stars or gas clouds made out of regular protons and neutrons, it had to be something else completely.

1.2 The candidates

As it became clear that dark matter was real, the question what it actually was naturally arose. The gas and dark planets and stars had been ruled out, especially after it was shown that it could not consist of baryons. The fact that it remains in spread out halos around galaxies and that it was not detected at all yet meant that it must interact very weakly with regular matter. A natural guess was then that it could be some nonbaryonic subatomic particle.

The first subatomic particle suggested as a candidate for dark matter was the neutrino. It has all the right properties: it is not a baryon, stable, neutral and interacts very weakly with other matter. However, simulations of galaxy formation ruled that dark matter could not consist of a fluid of relativistic particles. As we will see later, if the universe is dominated by a relativistic fluid the collapse of perturbations into structure is suppressed, and if dark matter would be relativistic, or "hot ", this would still be the case now, and the large scale structure that is observed could never have formed. Therefore, dark matter needs to be nonrelativistic, or "cold", at late times.

The next main candidate, and still a serious contender, is an undiscovered Weakly Interacting Massive Particle, or WIMP. These are also neutral, stable particles that interact very weakly with regular matter, but as opposed to the neutrino they are taken to have large masses, so that they quickly become nonrelativistic as the universe expands. An important reason why these were such a popular candidate was that particles with exactly these properties were predicted by supersymmetric extensions of the standard model. Supersymmetry predicts that every particle has a superpartner which is a boson if the particle is a fermion and vice versa, but otherwise has all the same quantum numbers. This means that there can be a wide range of neutral, heavy particles in these theories, and constraints coming from the fact that the proton has not been found to decay generically make the lightest of these particles stable.
Another factor playing into their popularity is the so-called WIMP miracle. If a particle that only interacts through the weak force is produced in the early universe, and then freezes out and goes out of equilibrium through the expansion of the universe, its predicted abundance is within an order of magnitude of the dark matter abundance. This generated a lot of excitement, and WIMPs became the leading candidate for a while.

Thus, the search for these WIMPs begun. This took a number of forms: for instance, the LHC was not only constructed to find the Higgs boson, but also to look for the superpartners predicted to be the WIMPS. A more direct way of searching for them is to put a big vat of xenon under a mountain and wait until one of them hits a

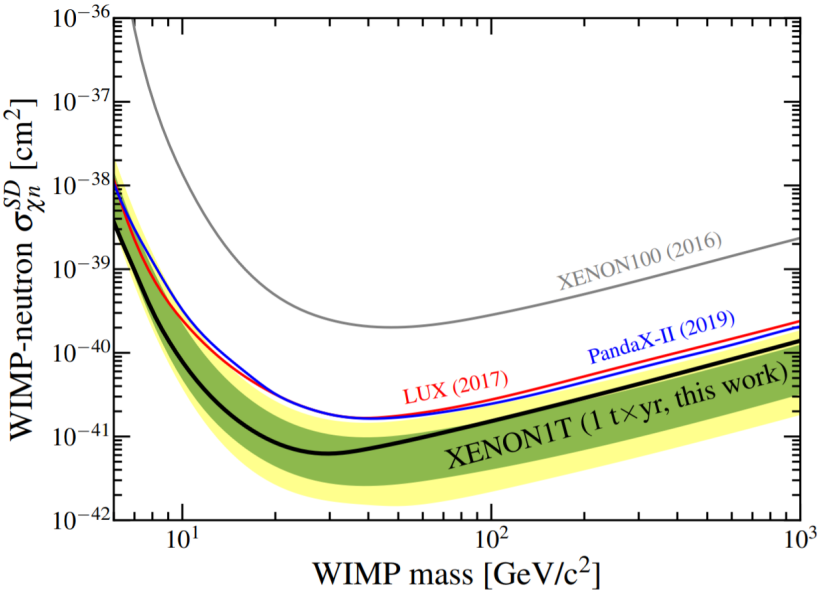

(a) Recent data from the WIMP search by the Xenon1t collaboration [13]. All WIMP-neutron cross-sections above the lines are excluded by the respective experiments. It can be seen the constraints have improved by orders of magnitude in the last years.

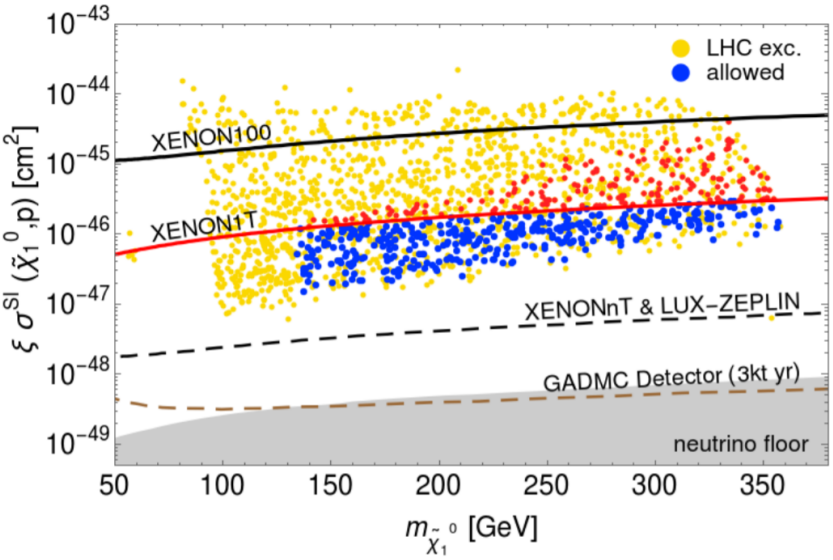

(b) In this figure, the cross-section of WIMPs predicted by a sampling of supersymmetric models coming from string theory are compared with results from the LHC and Xenon1T. It can be seen that most models are excluded, and that the ones that are still allowed can be ruled out by the next upgrade of the Xenon1T experiment. Taken from [14].

Figure 1.3

nucleus, causing scintillations that can be detected.

After twenty years of searching, there are still no signs of WIMPs today. This does not mean that they are ruled out as dark matter candidates, but the situation is becoming slightly worrying. The models that produce the WIMP miracle have been ruled out, and the same goes for many others. In figure 1.3 the latest results of the Xenon1t collaboration are shown, together with a number of models for WIMPs where the coupling constants have been sampled from supersymmetric theories coming from certain compactifications in string theory. These are by no means all possible models, but the picture is clear: there is no evidence yet, and the available parameter space is shrinking rapidly through the LHC and Xenon1T constraints.

Another option for subatomic particles making up dark matter are light scalars, of which the axion is the most prominent candidate. Axions are predicted by the Peccei-Quinn mechanism, which is proposed as the solution to the strong CP-problem, explaining why the strong force only violates CP-symmetry very weakly. As opposed to the WIMPs, they are very light, neutral particles, but they can form through mechanisms that ensure they become nonrelativistic early on [15]. Similarly as for the WIMPs, experiments are being conducted to look for them and they have not yet been found, but they are certainly not ruled out yet [1].

Other than having dark matter be some new particle, another possibility is that the measured effects can be explained by a modification of the laws of gravity. In this proposal, Newton's second law is not valid any more at very small accelerations, but gets modified such that instead of $F = ma$, we have $F = ma^2/a_0$. In this case of modified Newtonian dynamics (MOND), the flattening of the rotation curves arises naturally, without assuming any dark matter halo at all. When more general galactic dynamics like the Tully-Fisher relation between the luminosity and rotational velocity of spiral galaxies also turned out to be explained by this framework, a lot of enthusiasm was generated. However, MOND turns our not to fare too well at larger sizes than galaxies: the dynamics of clusters still require some form of other dark matter, and it also has a hard time explaining the cosmological evidence. It is also rather nontrivial, yet claimed to be possible, to write down a theory that has this type of behaviour while still being consistent with the measured expansion of the universe and solar system tests of gravity.

Another blow to MOND, or any theory hoping to explain dark matter as some non-material effect, was the observation of the bullet cluster in 2006. This consists of two clusters of galaxies, shown in figure 1.4, that have just collided and passed though each other. Most of the visible matter in the system is in clouds of gas that,

Figure 1.4: The bullet cluster, in which dark matter found through lensing is shown in purple and regular matter found by x-ray observations shown in pink. We see the two separate right in front of our eyes [16].
Figure credit: X-ray: NASA/CXC/CfA/ M.Markevitch et al.; Lensing Map: NASA/STScI; ESO WFI; Magellan/U.Arizona/ D.Clowe et al. Optical image: NASA/STScI; Magellan/U.Arizona/D.Clowe et al.

once they collided, interacted significantly with each other and slowed each other down. The gas got heated up and, as a result, emitted x-rays that were measured and shown in pink in the figure. It was also studied where most of the mass in this system was through lensing, and it turned out that most of the mass, shown in purple, had not undergone any slowing and passed right through the other cluster. As most of the visible mass of the system is in the clouds, this must be caused by dark matter, which does not get slowed down by electromagnetic interactions. We see the separation between dark and regular matter happening right in front of our eyes, and this is very hard for a theory like MOND to explain, and at the same time arguably the strongest proof of the existence of dark matter yet.

1.3 Primordial Black Holes as a solution

The candidate for dark matter we are concerned with in this thesis are primordial black holes (PBHs). These are black holes that form during the first second of the universe, as opposed to the "regular" black holes which form from supernovae at the end of the life of massive stars and can only occur a few hundred millions years into the universe at the earliest.
During this first second, the density of the universe is extremely high, and large enough fluctuations in it can cause a region to stop expanding and instead collapse gravitationally and form a black hole. This was first realised by Novikov and Zel'dovich in the 1960s, even though they did not use the term black hole yet[4]. The idea was further worked out on by Hawking and his PhD student Carr, who produced a number of papers on them in the early 1970s, working out their basic properties [3, 17, 18].

For instance, it was realised that they could form with any mass depending on the size of the overdensity that collapsed, including masses much smaller than those of black holes forming during stellar collapse. This meant that the Hawking radiation which was being proposed at the same time might actually be measurable if these very tiny black holes existed, so it should come as no surprise that Hawking in particular was very interested. Furthermore, since black holes formed in supernovae can only be on the order of a solar mass at the lightest [6], any measurement of a lighter black hole will mean a discovery of a PBH, as no other mechanisms are known for their production.

It was also realised that they mostly form at the same scale as the Hubble radius, meaning that the lightest PBHs form first, and the heaviest form latest. This is because the Jeans length, the minimal length for an overdensity to collapse instead of oscillate and disperse, is of the order of the Hubble radius in the radiation era, and hence only regions of this size can collapse [17][1]. Another key observation, already made by Novikov and Zel'dovich was that PBHs have to be very rare during the radiation era when they form. The energy in the radiation dominated fluid decays as a^{-4} as the universe expands, because it gets both diluted and redshifted. The PBHs however only dilute, and hence the energy density in them only decays as a^{-3}. This means that the current density of PBHs that form at time t, Ω_{PBH}, is related to the density at formation, β, by:[2]

[1] If a sufficiently large overdensity of a super-Hubble size forms, a primordial black hole of super-Hubble size would form. Such a black hole would not collapse, but instead it would encompass the whole Universe, inside which the expansion would continue. Since large super-Hubble regions are required for the formation of such black holes, we expect that their formation will be suppressed with respect to the sub-Hubble ones. Nevertheless, their formation probability will be non-vanishing. We leave a more detailed estimate for the probability of their formation for future work.

$$\Omega_{\rm PBH} \simeq \beta\Omega_{\rm r}(1+z) \sim 10^6\beta\left(\frac{t}{1{\rm s}}\right)^{-1/2} \tag{1.3.1}$$

where z is the redshift at which the PBHs form, and Ω_r is the density of radiation in the universe now. This means even a small fraction of PBHs at formation can have a significant density today, and because we know that when integrated over all masses $\Omega_{PBH} \leq \Omega_{DM}$, this places stringent constraints on β.

1.4 Current constraints on PBHs

The idea that dark matter might consist of compact, dark objects has been considered for a long time. These Massive Compact Halo Objects (MACHOs) might seem much more natural candidates for dark matter than WIMPs , but early observations were not kind to them. The main way to measure the abundance of MACHOs is to look at how they bend the light from stars, quasars or gamma ray bursts passing through the halo of the Milky Way by gravitational lensing. Starting in the late 1980s, there have been many surveys looking for this, and while they observed a small number of events it was too little for all the dark matter in the halo to consist of MACHOs of a broad mass range[19]. As it became accepted that dark matter was nonbaryonic, attention shifted towards unknown elementary particles as candidates.

However, with the lack of success these particle models have had in the past 20 years, the constraints on the PBH abundance from lensing do not look that bad at all. Because PBHs form in the first second of the universe, they are already nonbaryonic when nucleosynthesis happens three minutes in, and therefore avoid this constraint where the other MACHOs fail. A recent summary of the constraints on the current abundance of PBHs is shown in figure 1.5.

From this figure it seems that there are no windows left in which PBHs of a single mass can make up all of dark matter. However, whereas the constraints coming from lensing, the large scale structure and the photon background are seen as strong, the indirect and accretion constraints are a lot less certain. For instance, the NS constraint at around 10^{20} to 10^{24} g comes from the fact that light PBHs will get captured by neutron stars and quickly swallow them. Then, the observation of old enough neutron stars places constraints on the PBH fraction. These are however very dependent on the dark matter density at the centres of galaxies where these neutron stars reside. This value is not very well known, and the one used in the original study has been disputed[2]. Also, this picture is only for monochromatic distributions, which is where dark matter is made of PBHs with only a single mass. For broader distributions, it is possible for wider regions where the constraints are

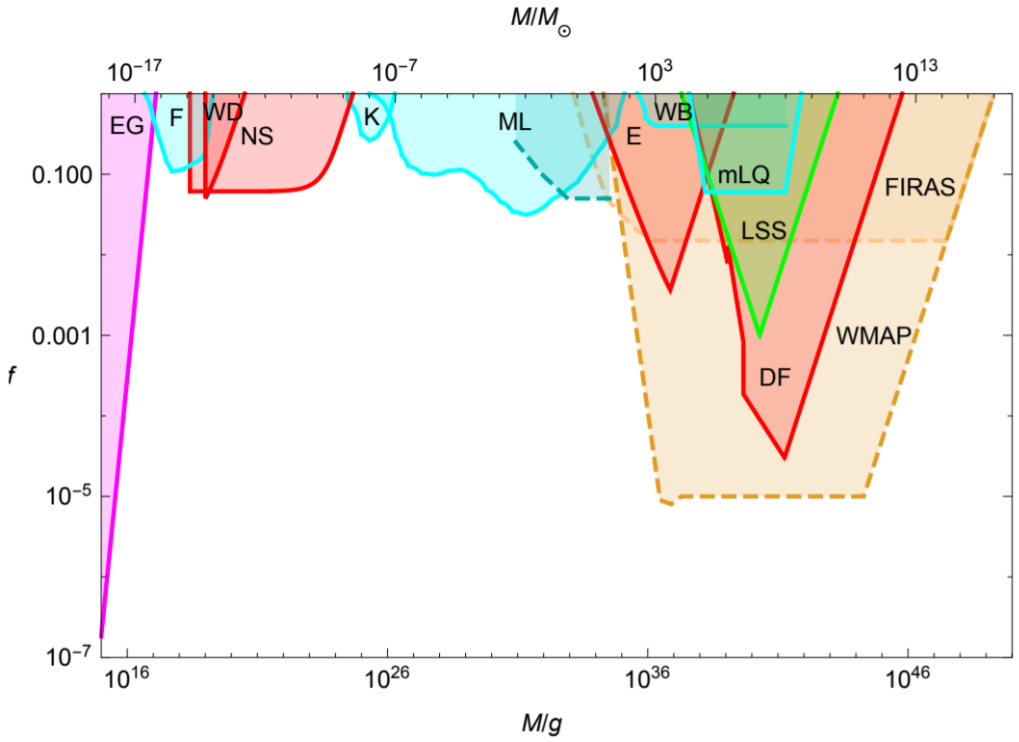

Figure 1.5: The current constraints on the fraction of dark matter that can consist of PBHs with mass M, for a monochromatic distribution. Coloured regions are excluded, with the blue regions being excluded by lensing surveys, the red by indirect observations, the yellow by accretion effects on the CMB, the green by the distribution of the large scale structure and the pink by the non-observation of hawking radiation of PBHs in the extragalactic photon background. Taken from [2].

weak to allow enough PBHs.

In the end, it turns out there are still three windows in which PBHs can make up all of dark matter [20]. The first are subatomic PBHs, with a mass of around $10^{17}g$, and an event horizon of around $10^{-11}cm$. Furthermore, there are sublunar black holes with a mass of less than $10^{24}g$, a range that might be open up to $10^{20}g$ if the neutron star constraints are not to be trusted. This is slightly less than the mass of the moon, hence the name. Lastly, there are intermediate black holes with masses of $1 - 10^3 M_\odot$. These could also make up the black holes found colliding by LIGO.

Up to now we have only considered PBHs as the solution to the dark matter problem. However, this is not the only reason why they are interesting. They might also

explain where the black holes we see colliding in LIGO come from, or might be the seeds of the supermassive black holes in the centres of galaxies, explaining their huge mass since PBHs can form with almost any mass.

There is one further observation that is relevant to PBHs, namely that all perturbations that we know of in the early universe are very small. The temperature fluctuations in the CMB are of the order 10^{-5}, and the distribution of galaxy clusters is extremely homogeneous on very large scales. For a PBH to form, we need large fluctuations, so this poses a problem. For any significant formation to occur, some kind of enhancement of the fluctuations on small scales is necessary. It is simply not known how homogeneous the early universe was at very small scales, so this enhancement is not excluded, but there is also certainly no evidence for it. How large exactly these fluctuations have to be is a question we will spend most of this thesis answering.

1.4.1 SVT decomposition

To look at what kind of fluctuations are needed to form PBHs, we first need to know how to describe fluctuations in the early universe in general. The main quantities of interest describing the state of the universe are the metric and stress-energy tensor. As mentioned before, for a PBH to form we need a region that has a large density fluctuation, and for this from the Einstein equation that relates density to curvature, we can already guess we will need significant curvature fluctuations. Taking into account the symmetry of the metric and stress-energy tensor we can write them in a general perturbed form as:

$$ds^2 = -(1+2\Phi)\mathrm{d}t^2 + 2a(t)B_i\mathrm{d}x^i\mathrm{d}t + a^2(t)\left[(1-2\Psi)\delta_{ij} + 2E_{ij}\right]\mathrm{d}x^i\mathrm{d}x^j \tag{1.4.1}$$

and

$$\begin{aligned} T^0_0 &= -(\overline{\rho} + \delta\rho) \\ T^0_i &= (\overline{\rho} + \overline{p})av_i \\ T^i_0 &= -(\overline{\rho} + \overline{p})\left(v^i - B^i\right)/a \\ T^i_j &= \delta^i_j(\overline{p} + \delta p) + \Sigma^i_j \end{aligned}, \tag{1.4.2}$$

where $\bar{\rho}$ and $\bar{p}$ are the background density and pressure. There are a lot of different perturbations in these equations: the potentials Ψ and Φ, a spatial vector perturbation B_i and a symmetric 3-tensor E_{ij} are the metric perturbations, and in the stress-energy tensor we have the density perturbation $\delta\rho$, pressure perturbation δp, momentum density perturbation v_i and anisotropic stress Σ^i_j : 10 degrees of freedom in both the metric and stress-energy tensor. Fortunately, we do not have to keep

track of all these quantities, in fact, it turns out we only have to focus our attention on one.

First of all, we see all sorts of different perturbations entering as scalars, spatial vectors or spatial 2-tensors. For instance, the metric perturbation Ψ is a scalar, and B_i is a 3-vector. We can fully decompose the metric perturbations into 4 scalars, 2 transverse vectors and a transverse and traceless tensor.

Then by studying the equations of motion it turns out the scalars, vectors and tensors do not mix at linear order [21]. Therefore, we can treat all of these perturbations separately. We are only interested in the scalars, since the density perturbation is a scalar and is hence only sourced by the vectors and tensors at second order. The vector modes also decay quickly with the expansion of the universe and are not produced by inflation.

Another great simplification comes from the fact that in general relativity, we are free to choose our coordinate system however we like, and we should still able to describe the universe with it. Choosing coordinates essentially is making the choice of a slicing of spacetime: we choose a certain stack of 3d-hypersurfaces and define these as having a given time. They should be defined such that the worldline of any particle travelling through spacetime threads all of these constant time hypersurfaces, but for the rest we are completely free to pick them however we like.

This choice has a large influence on all of the perturbations we just defined. Consider for instance an unperturbed homogeneous universe, with a density $\rho(t)$. If we now change our time coordinate in a space-dependent fashion as $t' = t + \delta t(\vec{x}, t)$, the density will no longer be constant for a given time. Perturbations appear, even though all we have done is change coordinates, which we are free to do; the physics should still describe a homogeneous universe. This goes to show that not all of these perturbations are physical. In fact, what we will turn out to be able to do is approximately the opposite. By choosing our coordinates in a smart way and under some assumptions, we will be able to set all but one of the scalar perturbations to zero, leaving us with only one function sourcing the density contrast and the PBH formation. This will be worked out in detail in chapter two. For now, we just assume there is only one scalar perturbation to deal with, given by ζ, which is a metric perturbation appearing as:

$$ds^2 = -dt^2 + a(t)^2 e^{2\zeta(t,\vec{x})} d\vec{x}^2. \tag{1.4.3}$$

From this, it can be seen that ζ is can be interpreted as a local volume perturbation: taking the determinant of the metric yields $-a^6 e^{6\zeta(\vec{x},t)}$, so the perturbation of the volume element $d^4x\sqrt{-g}$ at a given point goes like $e^{3\zeta(\vec{x},t)}$. Furthermore, the 3D Ricci scalar on the constant time hypersurfaces is given by $4\frac{\nabla^2}{a^2}\zeta$, so ζ can also be

interpreted as a spatial curvature perturbation. Applying the Einstein equations to this metric, we find the following equation, relating ζ to the density perturbation $\delta\rho(\vec{x},t) = \rho(\vec{x},t) - \bar{\rho}(t)$:

$$\frac{\delta\rho}{\rho_b}(r,t) \simeq -\frac{1}{a^2H^2}\frac{8}{9}e^{-5\zeta(r)/2}\nabla^2 e^{\zeta(r)/2} \tag{1.4.4}$$

where ρ_b is the background energy density, and it must be noted that we have assumed perturbations much larger than the Hubble radius, which is reasonable as we will see in the next chapter [22]. Because of homogeneity, both ζ and $\delta\rho$ only depend on the radial coordinate. Hence, we have found that ζ sources the density contrast $\delta\rho$, which again sources the PBH formation, as overdensities collapse to form them. Expanding this equation to first order in ζ we find the following:

$$\frac{\delta\rho}{\rho_b} \simeq -\frac{1}{a^2H^2}\frac{4}{9}\nabla^2\zeta. \tag{1.4.5}$$

This can be thought of as a relativistic version of the Poisson equation, and from this we can see that ζ can also be thought of as a gravitational potential.

By definition, ζ has zero expectation value, so the main measure of the fluctuations is the correlation function $\langle\zeta(\vec{x},t)\zeta^*(\vec{y},t)\rangle$. Assuming homogeneity, this will only depend on $r = |\vec{x}-\vec{y}|$. We will mostly use this in Fourier space, so it is useful to define the dimensionless power spectrum as:

$$\langle\zeta(\vec{x},t)\zeta^*(\vec{y},t)\rangle = \int_0^\infty \frac{dk}{k}\mathcal{P}_\zeta(k,t)\frac{\sin(kr)}{kr}. \tag{1.4.6}$$

With this definition, the power spectrum is given in terms of the Fourier modes of ζ as:

$$\mathcal{P}_\zeta(k,t) = \frac{k^3}{2\pi^2}|\zeta(k,t)|^2 \tag{1.4.7}$$

where because of the homogeneity of the theory all quantities are a function of the radial coördinate only. This Fourier transform for a spherical symmetric system is explicitly worked out in section 3.6.

1.4.2 Naive criteria for PBH formation

In this section, we sketch the usual calculation of the primordial black hole fraction in the universe [23, 24, 25, 26, 27]. The main quantity describing this, which we will spend a lot of effort calculating in this thesis is $\beta(M)$, defined as the fraction of the energy of the universe that is in PBHs of mass M at the moment they form:

$$\beta(M) = \frac{\rho_{PBH}(M)}{\rho_{tot}}|_{t=t_{formation}}. \tag{1.4.8}$$

Usually, it is assumed that a PBH forms if either ζ or the overdensity $\delta\rho/\rho$ is bigger than some threshold. The input for these critical values has mostly come from simulations of PBH formation, and the correct way of stating the criterion is still a highly contentious topic. Most commonly, a critical overdensity $\delta\rho_c$ is used in the literature, but this calculation is also sometimes presented with a ζ_c, which we will follow here for ease of connecting to the previous and later parts. The fraction of the universe in PBHs of mass M is then equal to the probability that ζ is greater than ζ_c in a region that, if it collapses, forms a PBH with mass M.

For ζ then a Gaussian probability distribution is assumed. The variance is given by the power spectrum, yielding:

$$P(\zeta) = \frac{1}{\sqrt{2\pi\mathcal{P}_\zeta}} e^{-\frac{\zeta^2}{2\mathcal{P}_\zeta}}. \tag{1.4.9}$$

In general though, the problem is that both the overdensity and curvature perturbation are local quantities, but the mass of the PBH that forms depends on the size of the collapsing region. To account for this, the perturbation is smoothed below a certain scale R. What this means in practice is that instead of $\zeta(\vec{x}, t)$, the variable used is:

$$\zeta(R, \vec{x}, t) = \frac{1}{V} \int d\vec{x}' \zeta(\vec{x}', t) W(|\vec{x} - \vec{x}'|/R) \tag{1.4.10}$$

where W is called the window function, which implements an averaging over perturbations on all scales smaller than R. V is a normalization factor determined by the volume of the window function. This function is nonunique: Gaussians and step functions have both been considered in the literature, and give significantly different answers. The smoothened power spectrum is then given by:

$$\sigma^2(R) = \int_0^\infty W^2(kR)\mathcal{P}_\zeta(k). \tag{1.4.11}$$

Then, the probability for a region of physical radius R to collapse and form a PBH is given by:

$$P(R) = \int_{\zeta_c}^\infty P(\zeta)d\zeta = \int_{\zeta_c}^\infty \sqrt{\frac{1}{2\pi\mathcal{P}_\zeta(R)}} e^{-\frac{\zeta(R)^2}{2\mathcal{P}_\zeta(R)}} \tag{1.4.12}$$

Now as PBHs form at horizon crossing, the mass can be related to the radius of the collapsing region. This will be worked out in detail later, for now the point is that we can find a function $R(M)$, allowing us to solve the above integral and get:

$$\beta(M) = \frac{1}{2}\text{erfc}(\frac{\zeta_c}{2\mathcal{P}_\zeta(R(M))}) \tag{1.4.13}$$

Where $\text{erfc}(x)$ is the complimentary error function, defined as

$$\text{erfc}(x) = \frac{2}{\sqrt{\pi}}\int_x^\infty dt e^{-t^2}. \tag{1.4.14}$$

This is the expression for β often seen in literature, but there are some problems with it. First of all, there is no unique way to do the smoothing, and different ways produce different results. Secondly, this calculation feels a bit naive: in the early universe, $\zeta(\vec{x}, t)$ is a field, in fact during inflation even a quantum field. In a full treatment of these fluctuations an expression like $\int d\zeta$ just does not make sense: the integral should be replaced by a path integral over all profiles for ζ. Furthermore, in this framework it is not completely clear which mass a PBH will eventually have if the perturbation is great enough to form a PBH on multiple scales.

In this thesis, we will try to improve on this calculation by doing it from first principles, taking the field-theory nature of it into account and using a different criterion for PBH formation, based on recent numerical studies.

1.4.3 Muscos criteria

Last year, Ilja Musco published two papers, one together with Cristiano Germani, in which the precise criteria for PBH formation were carefully determined using numerical simulations of PBH formation, with the aim of clearing up the large amount of confusion that had arose because many studies used different methods, approximations and implementations [5, 22]. We will use their results as the criteria for PBH formation, although it seems unlikely that this will end all discussion surrounding the topic. As it turns out, the right variable to use is the compaction function $\mathcal{C}$, defined by:

$$\mathcal{C}(R, t) \equiv \frac{2G\delta M(R, t)}{R(R, t)}. \tag{1.4.15}$$

This is a nonlocal quantity, defined for a region of radius R at time t, with $R(r, t) = are^{\zeta(r,t)}$ the physical radius of the sphere. $\delta M(R, t)$ is the excess mass in the region, defined as:

$$\delta M(R, t) = 4\pi\int_0^R dR'\delta\rho(R')R'^2 dR' \tag{1.4.16}$$

where $\delta\rho$ is the perturbation of the energy density.

A PBH will then form from a region of radius R if:

- $\mathcal{C}(R,t) > C_c$
- $\mathcal{C}(R,t)$ is at its maximum , so $\partial_R \mathcal{C}(R,t) = 0$.

From numerical simulations it was found that the actual value of $\mathcal{C}_c$ depends slightly on the shape of the overdensity. However, this dependence is greatest for shapes that have very steep density gradients like a step function overdensity profile. We expect these perturbations to be much rarer than smoother profiles, and since $\mathcal{C}_c$ is greater for them anyway we will ignore them and take the representative value $\mathcal{C}_c = 0.45$. For a full treatment however, we would like to take the shape-dependence into account and this is certainly interesting for future work.

Furthermore, in Musco's papers the first criterion is not only expressed in terms of $\mathcal{C}$, but also in terms of another nonlocal perturbation measure δ. They are equal at the maximum of $\mathcal{C}$ in the long wavelength approximation, and since PBH formation happens precisely at this scale the two ways of expressing the criterion are equivalent.

We note that the second criterion tells us the scale at which a given perturbation collapses to a PBH, so the radius of the region that collapses is always well-defined by this.
For implementing these criteria, we need to know how to determine $\mathcal{C}$ from the perturbations in the early universe, and what kind of probability distribution results from this. To do this, in the next chapter we will study the primordial perturbations and what is commonly accepted to be their source, inflation, so that in the end we can relate $\mathcal{C}$ to these quantities and determine the amount of PBHs that form from any theory of the perturbations in the early universe.

Chapter 2

Cosmological perturbation theory

In this chapter we study the source of the fluctuations in the early universe that seed the PBHs in detail, and in particular we will look at inflation, the most accepted theory of how these came to be. It was introduced in the 1980s to solve a number of problems with the traditional hot big bang theory [28, 29, 30], and has been consistent with experiments ever since. In the first parts of this chapter we will follow [21] closely, but use the notation of [31] and [32].

2.1 Inflation

2.1.1 Why inflation

The first problem solved by inflation is the horizon problem. In our universe we have the comoving horizon, which is the maximal distance a light ray could have travelled since the big bang. This is also exactly the amount of conformal time that has passed since the beginning of the universe. Two points separated by more than it can never have been in causal contact, since they have had no time to exchange information. It is given by:

$$\tau = \int_0^t \frac{dt'}{a(t')} = \int_0^a d\ln(a)\frac{1}{aH}. \tag{2.1.1}$$

Here, $\frac{1}{aH}$ is a very important quantity called the comoving Hubble radius, which plays a large role in inflation. Even though it is a comoving quantity, we will also often just call it the Hubble radius, but note that it is not a physical, but a coordinate distance. By the Friedmann equations its evolution is given by:

$$\frac{1}{aH} = H_0^{-1} a^{\frac{1}{2}(1+3w)}. \tag{2.1.2}$$

For a universe dominated by a component with $\omega > -\frac{1}{3}$, the comoving Hubble radius only increases with time. This means the integral in equation 2.1.1 is also increasing, so the horizon also increases. In other words, the size of patches of the universe that are in causal contact with each other are always increasing. As for both a radiation and matter dominated one has $\omega > -\frac{1}{3}$, this is the case for the standard hot big bang model. This poses a problem when looking at the CMB however.

The CMB is incredibly homogeneous: the temperature fluctuations are only of the order 10^{-5}. It was emitted 380.00 years after the big bang, so the particle horizon was a lot smaller than today. This means that perturbations on the largest scales we see in the CMB today, which stretch across the entire visible universe, were far outside the horizon when the CMB was emitted. However, they still have the same temperature despite never having been in causal contact with each other. There are even significant correlations between the temperature fluctuations on scales that were far outside of the horizon at the time of emission. The question of how this is possible is called the horizon problem.

Another reason to introduce inflation is the flatness problem. As mentioned before, recent CMB and large scale structure measurements have found the global curvature of the universe, κ, to be very small. This poses a problem because the amount of energy in the curvature of the universe, Ω_κ, only decays as a^{-2} when the universe expands. In particular, it behaves like $\frac{1}{a^2H^2}$, so it depends on the comoving Hubble radius. Cold matter and radiation scale as a^{-3} and a^{-4} respectively, so they decay much faster. This means that if Ω_κ is so small today, it must have been even smaller in the early universe. The flatness of the universe today requires an extremely fine-tuned flatness earlier, and there is no intrinsic reason why the curvature should be so small.

It turns out a solution to both of these problems is a period of accelerated expansion before the beginning of the radiation era, which is called inflation. During such a period, the comoving Hubble radius does not increase, but decreases with time. This means that two seemingly causally disconnected patches of the CMB were actually in causal contact before inflation, and could equilibrate, after which the Hubble radius decreased during inflation, making it seem as if they could never have been in contact. Put differently, the comoving horizon is now much larger than the comoving Hubble radius after inflation because the integral in 2.1.1 has a large contribution from the early times when the Hubble radius was much bigger. This means the horizon problem is solved. The flatness problem is also solved by such a period, because if the Hubble radius decreases, the curvature contribution to the universe also decreases. Hence, a period inflation automatically drives the universe towards the observed flatness.

Inflation does not only solve these problems, but also gives us the source of the fluctuations on all scales in the universe, because of the period of rapid, accelerated expansion. As we will see, quantum fluctuations get blown up to huge scales during inflation and become the seeds of all the structure we see today. These also seed the overdensities that might collapse to form PBHs, so it is of great interest to us to investigate them.

2.1.2 Single scalar field inflation

Then, the question is what could cause such a period of rapid expansion. The condition of having an accelerated expansion is equivalent to the universe being dominated by a fluid with equation of state $\omega < -\frac{1}{3}$, as can be seen from the second Friedmann equation 1.1.6.

The most common way that this behaviour is produced is by having the universe be dominated by the potential energy of a single scalar field ϕ, the inflaton. The action describing this theory is:

$$S = \int \mathrm{d}^4x\sqrt{-g}\left[\frac{1}{2}R + \frac{1}{2}g^{\mu\nu}\partial_\mu\phi\partial_\nu\phi - V(\phi)\right]. \tag{2.1.3}$$

Assuming a homogeneous FLRW background such that $\phi = \phi(t)$, the equation of motion for ϕ becomes:

$$\ddot{\phi} + 3H\dot{\phi} + \frac{dV}{d\phi} = 0. \tag{2.1.4}$$

Calculating the energy-momentum tensor from this action yields that it takes a perfect fluid form with: [21]

$$\omega_\phi = \frac{\dot{\phi}^2 - 2V(\phi)}{\dot{\phi}^2 + 2V(\phi)} \tag{2.1.5}$$

from which it can be seen that for a large enough potential $V(\phi)$, ω can actually be negative and small enough for accelerated expansion.

The potential that does the job is shown in figure 2.1. The inflaton starts off at high values of the potential, and then rolls down the potential slow enough such that the potential energy stays dominant over the kinetic energy for a long enough time to solve the problems, until it eventually settles down at the minimum.
By the second Friedmann equation 1.1.6, the condition that $\ddot{a}$ is positive is equivalent to having that

$$\frac{3}{2}(\omega_\phi + 1) < 1 \tag{2.1.6}$$

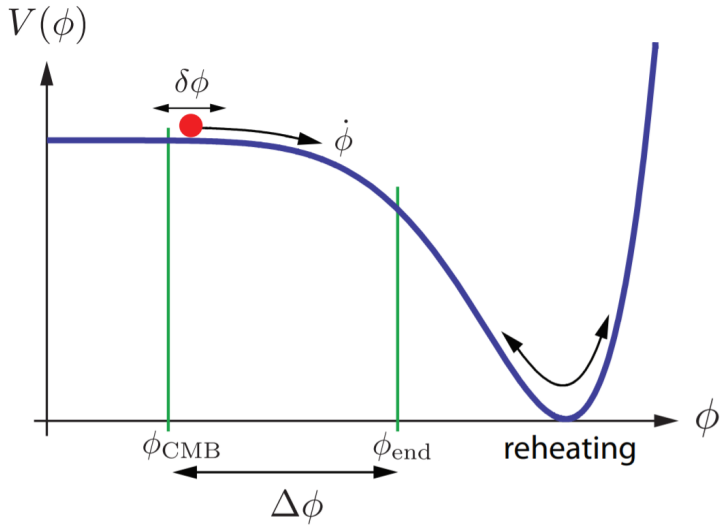

Figure 2.1: The potential for slow roll inflation: the inflaton starts on the right, and rolls down the potential slow enough such that the potential energy keeps dominating. Figure from [21].

By the expression for ω_ϕ and the second Friedmann equation this can be expressed in terms of $\dot{\phi}$ and $\dot{H}$, namely in terms of the first slow roll parameter, which is defined as:

$$\epsilon \equiv -\frac{\dot{H}}{H^2} = \frac{\dot{\phi}^2}{2H^2}. \tag{2.1.7}$$

The condition 2.1.6 then becomes $\epsilon < 1$. To remain in this state long enough, the acceleration of the field must also be small. This is determined by the smallness of the second slow roll parameter, η, defined by:

$$\eta \equiv \frac{\dot{\epsilon}}{\epsilon H} = -\frac{\ddot{\phi}}{H\dot{\phi}}. \tag{2.1.8}$$

$|\eta| < 1$ ensures that ϵ does not change rapidly, which could end the domination of potential energy. If both ϵ and η are small, slow roll inflation takes place, and the accelerated expansion of the universe can be sustained for a long enough time to solve the flatness and horizon problems. As $\dot{\phi}$ is very small, we have $\omega \approx -1$, and this means the scale factor grows exponentially, meaning H remains constant. This is all approximate, as ϵ and H both slowly change as the inflaton rolls down the potential.

The above discussion is very phenomenological: we simply assumed the existence of a scalar field with nice properties, and gave no further motivation. There are many different potentials that can be chosen to fulfil the slow roll conditions, and there

are even more alternative models of inflation with multiple fields, modifications to gravity and still there are many more models. Although the concept of inflation in general does make predictions that can be tested, it is very hard to distinguish these different models, and this is in fact one of the reasons why we are so interested in PBHs: their formation depends on the small scale predictions of these models that can not be conceivably tested any other way.

2.2 Cosmological perturbations for slow roll inflation

In the next sections, we will calculate what the fluctuations predicted by single field, slow roll inflation are. For this, we first need to study cosmological perturbations more carefully than before to see how to describe these fluctuations, also for other theories of inflation.
We look at a scalar field in a FLRW background, and study small perturbations around the homogeneous solution. This means we have:

$$\phi(\vec{x},t) = \bar{\phi}(t) + \delta\phi(\vec{x},t), \tag{2.2.1}$$

$$g_{\mu\nu}(\vec{x},t) = \bar{g}_{\mu\nu}(t) + \delta g_{\mu\nu}(\vec{x},t) \tag{2.2.2}$$

and

$$T_{\mu\nu}(\vec{x},t) = \bar{T}_{\mu\nu}(t) + \delta T_{\mu\nu}(\vec{x},t). \tag{2.2.3}$$

As discussed in chapter 1, we can limit ourselves to the scalar perturbations for looking at PBH formation. The scalar sector of the perturbed metric is given by:[21]

$$\mathrm{d}s^2 = -(1+2\Phi)\mathrm{d}t^2 + 2a(t)\partial_i B \mathrm{d}x^i \mathrm{d}t + a^2(t)\left[(1-2\Psi)\delta_{ij} + 2\partial_i\partial_j E\right]\mathrm{d}x^i \mathrm{d}x^j \tag{2.2.4}$$

where Ψ, Φ, B and E are the four scalar degrees of freedom.
The perturbed stress-energy tensor is given by:

$$\begin{aligned} T^0_0 &= -(\overline{\rho} + \delta\rho) \\ T^0_i &= (\overline{\rho} + \overline{p}) a v_i \\ T^i_0 &= -(\overline{\rho} + \overline{p})\left(v^i - B^i\right)/a \\ T^i_j &= \delta^i_j(\overline{p} + \delta p) + \Sigma^i_j \end{aligned} \tag{2.2.5}$$

with $\delta\rho$ and δp the density and pressure perturbation, and δq, which is defined such that $\partial_i \delta q = v_i$, is the momentum density.

As discussed in chapter 1, we have the freedom to choose any coordinate system or gauge we want in general relativity. The results we get should not depend on our choice, but the perturbations in the metric and stress-energy tensor can be gauge-dependent, like the density perturbation we saw before. This can of course be resolved by fixing a gauge immediately, but it then becomes very hard to compare calculations done in different gauges, and to relate these perturbations to observables. Fortunately, it turns out we can define a scalar perturbation that is gauge invariant and can be related directly to observables in linear perturbation theory. Because it is gauge invariant, we get the same results for it no matter which gauge we use to calculate it, and therefore predictions for the observables also do not depend on the gauge, so we lose the ambiguity. To define this scalar, we have to study how the perturbations change under gauge transformations. We consider an infinitesimal gauge or coordinate transformation:

$$\begin{aligned} t &\to t + \alpha \\ x^i &\to x^i + \delta^{ij}\partial_j \beta. \end{aligned} \tag{2.2.6}$$

Applying this transformation to the metric yields that the scalar metric variables transform as:

$$\begin{aligned} \Phi &\to \Phi - \dot{\alpha} \\ B &\to B + a^{-1}\alpha - a\dot{\beta} \\ E &\to E - \beta \\ \Psi &\to \Psi + H\alpha \end{aligned} \tag{2.2.7}$$

and the scalar matter perturbations $\delta\rho$, δp and δq transform as:

$$\begin{aligned} \delta\rho &\to \delta\rho - \dot{\bar{\rho}}\alpha \\ \delta p &\to \delta\rho - \dot{\bar{p}}\alpha \\ \delta q &\to \delta q + (\bar{\rho} + \bar{p})\alpha. \end{aligned} \tag{2.2.8}$$

From these, we can construct a variable that is a gauge invariant combination of matter and metric perturbations, namely the comoving curvature perturbation:

$$\zeta = \Psi - \frac{H}{\overline{\rho} + \overline{p}}\delta q. \tag{2.2.9}$$

From the transformations of Ψ and δq it is easy to see that this is invariant under gauge transformations. Another very important property of ζ is that for adiabatic perturbations it follows from Einstein's equations that ζ is constant on super-Hubble scales. Slow roll inflation produces only adiabatic perturbations, so outside of the Hubble radius, $\dot{\zeta} = 0$. This is the reason we are able to use a formula only valid far outside of the Hubble radius to describe what happens as perturbations cross it, and also the key to understanding the power spectrum predicted by inflation.

Perturbations on a given comoving scale were inside the comoving Hubble radius before inflation, then at some point during inflation when is was shrinking, they crossed it. They spent some time outside of the Hubble radius, until they re-entered it during the matter or radiation dominated era as it was growing again. Therefore, the perturbations that went on to source structure formation in the early universe had not changed since they exited the horizon during inflation. In other words, the initial conditions for the subhorizon evolution of the perturbations in our universe are set by the value they had when they first exited the horizon, and because their physical scale was much smaller at the time, these perturbations were given by the quantum fluctuations in the field.
A schematic of this process can be seen in figure 2.2

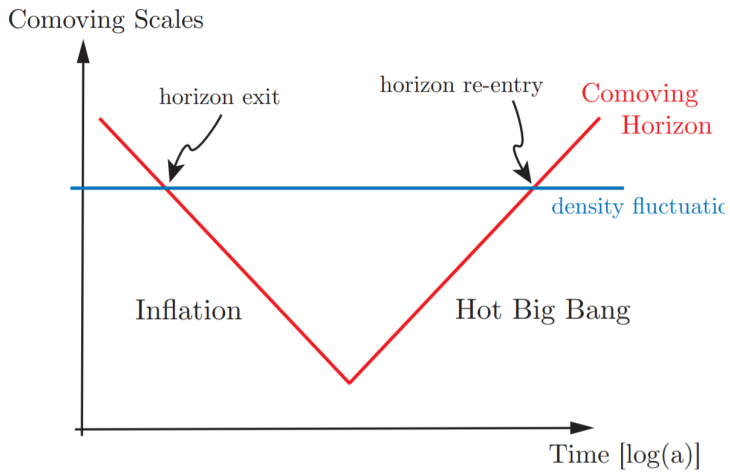

Figure 2.2: Schematic of the evolution of perturbations in the inflationary universe, Quantum fluctuations at early times exit the Hubble radius and remain constant afterwards, while the scale they are at gets stretched because of the expansion of the universe. After they re-enter in the radiation era, they source the fluctuations in the universe on all scales. Figure from [21].

2.3 The Mukhanov action

To calculate what the quantum fluctuations in ζ were like, we need to derive an action principle for it first. The gauge choice we will make to do this and for the rest of this thesis is to set all perturbations in the inflaton to 0, so $\delta\phi = 0$. Because the inflaton, which dominates the universe is unperturbed, we have $\delta q = 0$. Furthermore, we use the rest of our gauge freedom to set $E = 0$. This gauge is called the comoving gauge, and it is convenient for us because we want to track the perturbations through

inflation into the radiation era, when the inflaton is not around any more. If we would not gauge this degree of freedom away, we would need to translate the perturbations in it to those of the radiation fluid density, and it is unclear how to do so.

The action for the comoving curvature perturbation is most easily derived in the ADM formalism. As was mentioned before, part of choosing a gauge is specifying a certain slicing of spacetime into constant time hypersurfaces. The idea behind this formalism is that it allows us to split the information of the metric into that of the spatial metric on the hypersurfaces and into constraint fields determining the relation between them. The metric is therefore written as [33]:

$$\mathrm{d}s^2 = -N^2\mathrm{d}t^2 + g_{ij}\left(\mathrm{d}x^i + N^i\mathrm{d}t\right)\left(\mathrm{d}x^j + N^j\mathrm{d}t\right). \tag{2.3.1}$$

Here g_{ij} is the metric on a spatial slice, and the fields $N(\vec{x})$ and $N_i(\vec{x})$ are called the lapse and shift function. These will turn out to be constraint fields with no dynamics on their own, and they relate the spatial metrics on different slices with each other: N determines how quickly the time evolves, and the vector N_i determines how much the coordinates shift when going to a different slice.

In the comoving gauge, we will take $g_{ij} = a^2(t)e^{2\zeta}\delta_{ij}$. Note that this is only to first order equivalent to the definition of the perturbations in equation 2.2.7, but since we only calculate the action to second order only this is no problem, and with this form the calculations become a lot easier. Because we have gauged away all of the perturbations in the inflaton, we only need to look at the perturbed action for the metric to determine the dynamics. We can then calculate the action for ζ starting from the Einstein-Hilbert action:

$$S = \frac{M_p^2}{2}\int d^4x\sqrt{-g}R. \tag{2.3.2}$$

We can then substitute the ADM form of the metric into this action and expand up to second order in ζ. This yields an action only in terms of ζ, N and N_i. We can then solve the equations of motions given by this action for the lapse and shift, and plug the solutions back into the action. Then, after quite some more work one arrives at the following:

$$S = \frac{M_p^2}{2}\int \mathrm{d}^4x a^3 2\epsilon\left[\dot{\zeta}^2 - a^{-2}\left(\partial_i\zeta\right)^2\right]. \tag{2.3.3}$$

This was first derived by Mukhanov and others in the 90s [34]. Note that the first slow roll parameter $\epsilon = -\frac{\dot{H}}{H^2}$ shows up in this action, even though we have made no assumption of slow roll anywhere. To quantize this action, it is easiest to go to a

variable that will canonically normalise it, so that there is no time-dependent term in front of the kinetic term. This will put it in the form of a harmonic oscillator from which we know how to proceed. The right variable is called the Mukhanov variable, and it is defined by:

$$v \equiv z\zeta \tag{2.3.4}$$

where

$$z^2 \equiv a^2 \frac{\dot{\phi}^2}{H^2} = 2a^2\epsilon. \tag{2.3.5}$$

Now if we also switch to conformal time, we can write the action as:

$$S_{(2)} = \frac{M_p^2}{2} \int \mathrm{d}\tau \mathrm{d}^3x \left[\left(v'\right)^2 + \left(\partial_i v\right)^2 + \frac{z''}{z} v^2 \right]. \tag{2.3.6}$$

This can be seen as the action of a simple harmonic oscillator with a time-dependent frequency z''/z.
We then expand v into Fourier modes:

$$v(\vec{x}, \tau) = \int \frac{d^3k}{2\pi^3} v_{\vec{k}}(\tau) e^{i\vec{k}\cdot\vec{x}}. \tag{2.3.7}$$

Because of the homogeneity, the mode functions only depend on the norm of $\vec{k}$, denoted as k. By varying the action, the equation of motion for the modes v_k then becomes:

$$v_k'' + \left(k^2 - \frac{z''}{z}\right) v_k = 0. \tag{2.3.8}$$

This is known as the Mukhanov-Sasaki equation. To derive the evolution of the perturbation, this equation needs to be solved, which is quite hard in general because z''/z can be a complicated function of time. However, we will see that for certain backgrounds it is possible.

2.4 Quantization of cosmological perturbations

Next, we quantize this action by promoting v to an operator. Its conjugate momentum is then v', and hence the canonical commutation relations are:

$$[\hat{v}(\vec{x}, \tau), \hat{v}'(\vec{y}, \tau)] = i\delta^{(3)}(\vec{x} - \vec{y}). \tag{2.4.1}$$

We want to look at the Fourier modes, which we decompose into creation and annihilation operators by:

$$\hat{v}_{\vec{k}} = v_k(\tau)\hat{a}_{\vec{k}} + v_k^*(\tau)\hat{a}_{\vec{k}}^\dagger \tag{2.4.2}$$

which we would like to satisfy the canonical commutation relations:

$$\left[\hat{a}_{\vec{k}}, \hat{a}^{\dagger}_{\vec{k}'}\right] = (2\pi)^3 \delta^3\left(\vec{k} - \vec{k}'\right). \tag{2.4.3}$$

To satisfy both this and the canonical commutation relations for v and its momentum, one can show that we need Wrongskian of the mode functions v_k to be i:

$$W[v_k(\tau), v_k^*(\tau)] = v_k^{*'} v_k - v_k^* v_k' = i \tag{2.4.4}$$

This places one constraint on the mode functions v we will need later.

We will now solve the Mukhanov-Sasaki equation 2.3.8 in a de Sitter background ($\omega = -1$, H constant) to find the power spectrum. Even though slow roll inflation is not perfectly described by de Sitter because H is not actually constant, and a constant H would mean $\epsilon = 0$, the result can still be used to find the power spectrum. For this, we take ϵ to be non-zero despite H being constant. The result found by using this method agrees with the correct answer found by solving equation 2.3.8 for the actual, almost de Sitter background to first order in the slow roll paramters[32], so for simplicity we will only consider a de Sitter background. For $\omega = -1$ we have $a \propto -\frac{1}{\tau}$, so we get:

$$\frac{z''}{z} = \frac{a''}{a} = \frac{2}{\tau^2}. \tag{2.4.5}$$

This means the equation for the mode functions we need to solve is:

$$v_k'' + \left(k^2 - \frac{2}{\tau^2}\right) v_k = 0. \tag{2.4.6}$$

The solutions to this equation are given by:

$$v_k(\tau) = \alpha(k)\frac{e^{-ik\tau}}{\sqrt{2k}}\left(1 - \frac{i}{k\tau}\right) + \beta(k)\frac{e^{ik\tau}}{\sqrt{2k}}\left(1 + \frac{i}{k\tau}\right) \tag{2.4.7}$$

where $\alpha(k)$ and $\beta(k)$ are free complex parameters. We see that the mode functions are not unique: there are four undetermined real numbers. The requirement that the Wrongskian is i sets $|\alpha(k)|^2 - |\beta(k)|^2 = 1$, which fixes one of them. One more can be seen as an overall phase, which does not contribute to the power spectrum which goes like $|v(k,\tau)|^2$. This leaves two arbitrary, unspecified real numbers.

The freedom to choose these numbers is related to the fact that in curved spacetime, the vacuum is not uniquely defined. Making a choice for these therefore comes down to making a choice for a specific vacuum of the theory. One very common choice is to require that an observer far in the past, when all of the relevant modes were deep inside the horizon would see the vacuum of Minkowski space. Note that we

are doing this calculation in de Sitter space, so inflation has no beginning and this concept makes sense. If this observer sees no expansion, the equation for the modes becomes $v_k'' + k^2 v_k = 0$. Hence, we can impose the solution to this as a boundary condition at $\tau = -\infty$, so we require:

$$\lim_{\tau \to -\infty} v_k(\tau) = \frac{e^{-ik\tau}}{\sqrt{2k}}. \tag{2.4.8}$$

Together with the Wrongskian condition this implies that $\alpha(k) = 1$ and $\beta(k) = 0$. This choice of vacuum is called the Bunch-Davies vacuum, and is commonly used in the literature. There is a flaw in the reasoning above however: in the limit of $\tau \to -\infty$, the physical momentum goes to infinity as $a \to 0$. Therefore, gravity becomes strongly interacting, and as we are only working to second order in the perturbations the equations for the modes do not apply any more. It is possible to work around this and properly define a vacuum by only looking at states at finite times, the so-called adiabatic vacuum, but we will not be concerned with this and do our calculation in the Bunch-Davies vacuum for simplicity.

2.5 The power spectrum of slow roll inflation

We have now found the mode functions for slow roll inflation in de Sitter:

$$v_k(\tau) = \frac{e^{-ik\tau}}{\sqrt{2k}} \left(1 - \frac{i}{k\tau}\right). \tag{2.5.1}$$

To find the power spectrum for ζ, we recall that:

$$\mathcal{P}_\zeta = \frac{k^3}{2\pi^2} |\zeta(k,\tau)|^2 \tag{2.5.2}$$

and that $v = M_p \sqrt{2a^2\epsilon}\zeta$. Using all of these, and evaluating it at the first Hubble crossing we find:

$$\mathcal{P}_\zeta(k) = \frac{H_*^2}{4M_p^2 \pi^2 \epsilon_*} \tag{2.5.3}$$

where the subscript $*$ means that the quantity is evaluated at the Hubble crossing $k = aH$. This has no time-dependence any more because when it is outside the Hubble radius it remains constant. The perturbations only start evolving again when crossing it in the radiation or matter dominated era, and as we only look at the spectrum at Hubble crossing we can ignore this. Now because inflation is not described by a perfect de Sitter background, this quantity is not completely independent of k: ϵ and H slowly decrease during inflation, and smaller modes exit the horizon at later times, so every mode has a slightly different amplitude,

determined by the value of ϵ and H when it first crossed the horizon. This leads us to write the power spectrum as:

$$\mathcal{P}_\zeta(k) = \mathcal{P}_{\zeta *}(\frac{k}{k_*})^{n_s-1}, \qquad \mathcal{P}_{\zeta *} = \frac{H_*^2}{4\pi^2\epsilon_*}. \tag{2.5.4}$$

Here the deviation from scale invariance is parametrized by n_s being different from one, and k_* is some momentum scale, with the $*$ now meaning evaluated at the first Hubble crossing of k_*. It turns out that n_s can be expressed in the first and second slow roll parameters as:[21]

$$n_s = 1 - 2\epsilon - \eta. \tag{2.5.5}$$

Since these parameters are small in slow roll inflation, it predicts a power spectrum that has a slight deviation from scale invariance [35]. A scale invariant spectrum, also called the Zel'dovich spectrum, had already been introduced ten years earlier as a candidate to descibe our universe based on considerations from nucleosynthesis calculations, the entropy and the large scale structure [36]. The small deviation from scale invariance predicted by inflation has since been confirmed by the CMB data, with the latest results from the PLANCK satellite being [11]:

$$n_s = 0.965 \pm 0.004 \tag{2.5.6}$$

$$P_{\zeta *} = \left(2.101^{+0.031}_{-0.034}\right) \times 10^{-9}. \tag{2.5.7}$$

The success of this prediction is one of the reasons why inflation is the best-supported theory of what causes fluctuations in the early universe. However, for PBH formation, there is a problem: the amplitude of these fluctuations seems to be very small.

As the formation of PBHs requires a significant peak in the power spectrum, they cannot be produced in a universe described by just SR inflation: the perturbations on large scales are just too small to allow for large enough perturbations on small scales. Therefore, if PBHs are to be produced in the early universe, something else must be going on.

2.6 Beyond slow roll inflation

Slow roll inflation predicts an almost scale invariant spectrum of very small fluctuations, so there cannot be any large fluctuations at small scales. To get this enhancement of fluctuations that might form PBHs, we therefore need to look at other models. One way in which the power spectrum might become enhanced at small scales is if the inflaton enters a state of ultra slow roll (USR) during inflation. As the name suggests, during such a period the inflaton rolls down the potential

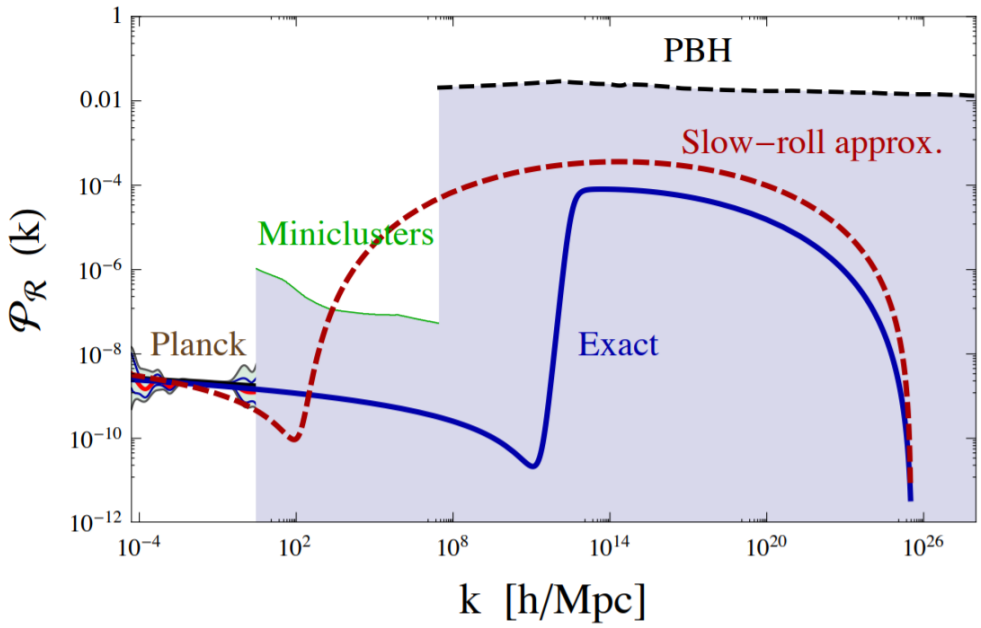

Figure 2.3: The power spectrum caused by a period of USR as found by Garcia-Bellido and Ruiz Morales in [37], calculated both in the slow roll approximation and exactly using numerics. In their notation, $\zeta = \mathcal{R}$.

even slower than during SR inflation, such that ϵ goes to zero, and the acceleration of the field, sourced by the second slow roll parameter η, becomes important. This can be caused by a flat region in the inflaton potential such as an inflection point.

Several of these models have been studied recently [37, 26, 38], and it has been shown that in this case the power spectrum is still given by equation 2.5.3, so it is still inversely proportional to ϵ. This means that it will grow significantly when ϵ approaches zero. These perturbations must be nonadiabatic, because it is no longer true that $\dot{\zeta} = 0$. It has been claimed that it is possible for this growth to only happen at small scales, and hence give rise to the enhancement that is both consistent with large scale constraints from the CMB and LSS yet is large enough on small scales to form PBHs[37].The power spectrum determined in this paper is shown in figure 2.3, where it is indeed clear that there is a significant enhancement on small scales.

Instead of trying to parametrize this or any other specific beyond slow roll theory of inflation, we will study power spectra that have enhancement on small scales in general. Our goal is then to develop a framework to calculate the PBH abundance

for any given theory. We will take the enhanced power spectra to have the form:

$$\mathcal{P}_\zeta(k,\tau) = \mathcal{P}_{SR}(k,\tau)(1 + Af((k-k_0)/a)) \tag{2.6.1}$$

Where $f(K-K_0)$ is a function that switches on above a physical scale K_0.

2.7 Evolution of mode functions in the radiation era

As PBHs can start to form when a perturbation re-enters the Hubble radius during the radiation era, it is useful to know how the perturbations evolve afterwards. We will find that they decay quickly, which means the assumption that PBHs only form right after Hubble crossing is valid.

When the universe is dominated by hydrodynamic matter, the derivation of the Mukhanov action can be generalised to: [34].

$$S_{(2)} = \frac{1}{2}\int \mathrm{d}\tau \mathrm{d}^3x \left[\left(v'\right)^2 - c_s^2\left(\partial_i v\right)^2 + \frac{z''}{z}v^2\right]. \tag{2.7.1}$$

Where c_s^2 is the speed of sound $\frac{dp}{d\rho}$ for adiabatic fluctuations. This enters because for a matter or radiation dominated universe, the scalar fluctuations are transported by sound waves in the cosmic fluid. Note that for the inflationary state we have $c_s^2 = -1$, in which case this reduces to the action seen previously. From this we have again the Mukhanov-Sasaki equation for the mode functions:

$$v_k'' - \left(c_s^2 k^2 + \frac{z''}{z}\right)v_k = 0. \tag{2.7.2}$$

In the radiation era we have that $\epsilon = \frac{3}{2}(\omega+1) = 2$, and hence $\frac{z''}{z} = \frac{a''}{a}$. We also have that $a(\tau) \propto \tau$, and $c_s^2 = \frac{1}{3}$,so the Mukhanov-Sasaki-equation reduces to:

$$v_k'' = -\frac{k^2}{3}v_k. \tag{2.7.3}$$

Solving this and switching back to ζ yields:

$$\zeta_{rad}(k,\tau) = \alpha(k)\frac{e^{ik\tau c_s}}{2a(\tau)\sqrt{2kc_s}} + \beta(k)\frac{e^{-ik\tau c_s}}{2a(\tau)\sqrt{2kc_s}} \tag{2.7.4}$$

where we have added some factors independent of τ to simplify our calculation later. This describes how the mode functions evolve in the radiation era. The factors of a come from switching back to ζ from v. Here we already see that these modes decay like a^{-1}. To connect this to the result of the mode functions during inflation, we need to match this form to the value of ζ when inflation ends, at $\tau = \tau_e$. If inflation ends during a slow roll phase, we then have $\dot{\zeta} = 0$. This might not be true in general for PBH-forming theories, so it might be interesting to see how this changes the

subhorizon evolution of the modes.
For now however, if $\zeta_0(k)$ is the mode frozen on superhubble scales predicted by inflation, the constants α and β are determined by requiring:

$$\zeta_{rad}(\tau_e, k) = \zeta_0(k) \tag{2.7.5}$$
$$\dot{\zeta}_{rad}(\tau_e, k) = 0 \tag{2.7.6}$$

Performing this matching for $\tau_e = 0$, we find that for modes inside the Hubble radius we have:

$$\mathcal{P}_\zeta(k, \tau) = \mathcal{P}_{\zeta,0}(k) \frac{\sin^2(k\tau/\sqrt{3})}{3k^2 a(\tau)^2} \tag{2.7.7}$$

Where $\mathcal{P}_{\zeta,0}(k)$ is the power spectrum coming from inflation. Hence, the power spectrum decays as $a^{-2} \propto \tau^{-2}$ inside the horizon, and the perturbation quickly disperses.

Chapter 3

The probability for the compaction function

In this chapter we calculate the probability distribution for the compaction function $\mathcal{C}$, so that we can calculate the probability that it is greater than the critical value in chapter 4. To get to this, we first calculate the distribution of the curvature perturbation, and then relate the two to each other.

As we saw in the last section, according to the theory of cosmological inflation perturbations in the early universe on all scales are sourced by quantum fluctuations that got blown up by a period of rapid expansion. This means that quantum effects are important for them, and we should take them into account. The quantum state of a system is completely described by its density matrix, which is the starting point of the calculations in this section.

3.1 The Wigner function

To calculate the probability that a PBH forms in a given region of space, we need to calculate the probability that a quantum field has a certain value: we need the probability distribution for a quantum field. This can be determined in a natural way from a field-theoretic extension of the Wigner function. To study its properties, we first introduce it in quantum mechanics. The Wigner function of a state is defined as:

$$W(x,p,t) = \frac{1}{2\pi}\int_{-\infty}^{\infty} dy \langle x + \frac{y}{2}|\rho(t)|x - \frac{y}{2}\rangle e^{-ipy} \tag{3.1.1}$$

where ρ is the density matrix of the state. This has the following properties that make it look a lot like a probability distribution on phase space:

$$\int_{-\infty}^{\infty} dpW(x,p;t) = \int_{-\infty}^{\infty} dy\langle x + \frac{y}{2}|\rho(t)|x - \frac{y}{2}\rangle\delta(y) = \langle x|\rho(t)|x\rangle \tag{3.1.2}$$

and similarly,

$$\int_{-\infty}^{\infty} dxW(x,p;t) = \langle p|\rho(t)|p\rangle \tag{3.1.3}$$

For pure states, these are just the wavefunctions of the state, so these are clearly probability distributions. We also have that $\int_{-\infty}^{\infty} dpdxW(x,p;t) = 1$ because $\mathrm{Tr}(\rho) = 1$. It seems like the Wigner function behaves as expected for a probability density. The only problem is that it is in general not positive: already for the exited states of a simple harmonic oscillator it is no longer positive on all of phase space. This means it can clearly not be interpreted as a probability in this case. Fortunately, there is a class of states for which it is always positive, the Gaussian states, for which the density matrix and hence also the Wigner function have the form of a Gaussian. These are also precisely the states that are produced during inflation, so we can use the Wigner function as a probability density on phase space for the state of ζ and its canonical momentum field Π. As these are fields, we need to study the Wigner function in Field theory.

3.2 Wigner function for Gaussian states in QFT

Defining the Wigner function unambiguously is harder in QFT than in quantum mechanics. The way in which time- and spatial dependence enters in its definition is very different, so there does not seem to be an obvious generalization. The way out of this is the functional Schrödinger picture[39], in which the two are separated from the onset. What this comes down to is that we first pick a given time, and then only look at the constant hypersurface of that time. Hence, we can describe the state of the field ζ by only looking at every point on the hypersurface: $|\zeta\rangle = \Pi_{\vec{x}}|\zeta(\vec{x})\rangle$. In this way we break covariance, but we have fixed our coordinates already anyway, so this is no problem. Using this separation of space and time the Wigner function can be defined as:

$$\mathcal{W}[\zeta,\Pi_\zeta,t] = \int \mathcal{D}\phi\langle\zeta + \frac{\phi}{2}|\rho(t)|\zeta - \frac{\phi}{2}\rangle \exp\{-i\int d\vec{x}\Pi_\zeta(\vec{x})\phi(\vec{x})\} \tag{3.2.1}$$

where the fields are only functions of position, so we can interpret $\mathcal{D}\phi = \Pi_{\vec{x}} d\phi(\vec{x})$. We then want to evaluate this for a Gaussian state, the states that describe inflation, and calculate the probability distribution of ζ from it. The density matrix of a Gaussian state in the functional Schrödinger picture is given by:[40]

$$\langle\phi|\rho(t)|\phi'\rangle = \mathcal{N}\exp\{-\frac{1}{2}\int d\vec{x}d\vec{y}[\phi(\vec{x})A(\vec{x},\vec{y},t)\phi(\vec{y}) + \phi'(\vec{x})B(\vec{x},\vec{y},t)\phi'(\vec{y}) \quad (3.2.2)$$

$$- 2\phi(\vec{x})C(\vec{x},\vec{y},t)\phi'(\vec{y})]. \quad (3.2.3)$$

Where A,B and C are functions defining the density matrix that follow the von Neumann evolution equation for it. For notational simplicity in the upcoming parts, we will see $\phi(\vec{x})$ as a vector and $A(\vec{x},\vec{y},t)$ as a matrix, so that we can define:

$$A\cdot\phi := \int d\vec{x}\phi(\vec{x})A(\vec{x},\vec{y},t) \quad (3.2.4)$$

which is again a vector, and with this product quantities like $\phi^T\cdot A\cdot\phi$ are scalars. We assume a homogeneous universe, so the operators must be symmetric.

We note that the density matrix must be Hermitian, so the expression should be invariant under at the same time complex conjugation and switching ϕ and ϕ', or transposing the operators if we see them as matrices. This means we must have $A^*(\vec{x},\vec{y}) = B(\vec{y},\vec{x})$ and $C^*(\vec{x},\vec{y}) = C(\vec{y},\vec{x})$. The normalization $\mathcal{N}$ can be determined from the requirement $\mathrm{Tr}(\rho) = 1$, but we will not specify it here: we will only properly normalise our probability at the last moment.
Filling this into the definition for the Wigner function, completing the square and integrating over ϕ yields:

$$W[\zeta,\Pi_\zeta] \propto \exp\{-\frac{1}{2}[\zeta^T\cdot\mathcal{O}_1\cdot\zeta + \zeta^T\cdot\mathcal{O}_3\cdot\Pi_\zeta + \Pi_\zeta^T\cdot\mathcal{O}_2\cdot\Pi_\zeta]\} \quad (3.2.5)$$

with:

$$\mathcal{O}_1 = \frac{1}{2}\left[A+B+2C-(A-B)\cdot(A+B-2C)^{-1}\cdot(A-B)\right] \quad (3.2.6)$$

$$\mathcal{O}_2 = 2(A+B-2C)^{-1} \quad (3.2.7)$$

$$\mathcal{O}_3 = -i[(A-B)\cdot(A+B-2C)^{-1} + (A+B-2C)^{-1}\cdot(A-B)]. \quad (3.2.8)$$

Because $A^* = B$ and $C = C^*$, these are real operators, and ζ and Π are real fields, so the Wigner function is manifestly nonnegative, and we can interpret it as the probability distribution on phase space for the state defined by A, B and C.

3.3 From power spectra to the Wigner function.

It is possible to express all the operators that enter the density matrix of a Gaussian state in terms of correlation functions of the field and its momentum, by noting that all expectation values of operators can be written in terms of the density matrix as:

$$\langle\zeta(\vec{x})\zeta(\vec{y})\rangle = \mathrm{Tr}[\hat{\rho}(t)\zeta(\vec{x})\zeta(\vec{y})]. \tag{3.3.1}$$

Using this, one can derive the following expressions: [40]

$$\langle\hat{\zeta}(\vec{x})\hat{\zeta}(\vec{y})\rangle = \frac{1}{2}\left(A_{\mathrm{H}} - C\right)^{-1}(\vec{x},\vec{y};t)' \tag{3.3.2}$$

$$\frac{1}{2}\langle\{\hat{\zeta}(\vec{x}),\hat{\Pi}(\vec{y})\}\rangle = -\frac{1}{2}\left(A_{\mathrm{H}} - C\right)^{-1}\cdot A_{\bar{\mathrm{H}}}(\vec{x},\vec{y};t) \tag{3.3.3}$$

$$\begin{aligned}&\langle\hat{\Pi}(\vec{x})\hat{\Pi}(\vec{y})\rangle \\ &= \frac{1}{2}\left[\frac{1}{2}A^{\dagger}\cdot\left(A_{\mathrm{H}} - C\right)^{-1}\cdot A + A\cdot\left(A_{\mathrm{H}} - C\right)^{-1}\cdot A^{\dagger} - C\cdot\left(A_{\mathrm{H}} - C\right)^{-1}\cdot C\right](\vec{x},\vec{y};t)\end{aligned} \tag{3.3.4}$$

Where A_H and $A_{\bar{H}}$ are the Hermitian and anti-Hermitian parts of A, which also determine B completely via $A^{\dagger} = B$. This means we can also take a given form of the power spectrum and momentum-field and momentum-momentum correlators as our input. This means we can work directly with the general enhanced power spectrum defined in chapter 2. What to choose for the momentum correlators is much harder to say in general. For slow roll inflation they are negligible, as $\Pi = \dot{\zeta} = 0$, but in other scenarios there is generally little known about their form.

There is no reason in principle for there to be a criterion just on ζ: the value of Π might also influence whether a PBH forms. For instance, it is conceivable that a PBH will not form even when the criterion for $\mathcal{C}$ is satisfied if $\Pi = \dot{\zeta}$ is such that the fluctuation will very rapidly decrease, causing it to disperse before it has fully collapsed. Therefore, in principle, we would also expect a criterion for Π to determine if a region will collapse to a PBH. As far as we know, there have been no numerical studies conducted investigating this. Therefore, we will only focus on the criterion for ζ. However, we hope that this will inspire numerical investigations into the effect of large momentum fluctuations on PBH formation.

3.4 Probability for ζ

From the Wigner function, we can calculate the probability distribution for ζ by:

$$P[\zeta] \propto \int \mathcal{D}\Pi W[\zeta,\Pi]. \tag{3.4.1}$$

Where again, we will only normalise the probability at the very last moment. We can perform the integral over Π most easily by switching to Fourier space. Because of the translation invariance the operators diagonalise:

$$P[\zeta] = \int \mathcal{D}\Pi \exp\{-\frac{1}{2}\int \frac{d\vec{k}}{(2\pi)^3}\zeta(\vec{k})\mathcal{O}_1(\vec{k})\zeta(-\vec{k})+\zeta(\vec{k})\mathcal{O}_3(\vec{k})\Pi(-\vec{k}))+\Pi(\vec{k})\mathcal{O}_2(\vec{k})\Pi(-\vec{k})\}, \tag{3.4.2}$$

where we have that $\zeta^*(\vec{k}) = \zeta(-\vec{k})$ and likewise for Π. We have these conditions because $\zeta(\vec{x})$ is real, so $\zeta(\vec{x})^* = \zeta(\vec{x})$. This also fixes the extra degree of freedom we have seemingly gained by the transformation because $\zeta(\vec{k})$ is now complex instead of real. Now assuming isotropy and a spherically symmetric perturbation $\zeta(\vec{x}) = \zeta(|\vec{x}|)$, all of the operators and fields in k-space depend only on on the norm of $\vec{k}$, which we denote by k. This means we have $\zeta(\vec{k}) = \zeta(k)$ so we can integrate over the angles, yielding:

$$P[\zeta] = \int \mathcal{D}\Pi \exp\{-\frac{1}{4\pi^2}\int dk k^2(\zeta(k)\mathcal{O}_1(k)\zeta(k)+\zeta(k)\mathcal{O}_3(k)\Pi(k)+\Pi(k)\mathcal{O}_2(k)\Pi(k))\}. \tag{3.4.3}$$

This also means that $\zeta^*(\vec{k}) = \zeta(-\vec{k}) = \zeta(|-\vec{k}|) = \zeta(k)$, so the Fourier transform of a spherical symmetric real function is also real. We can complete the square by transforming:

$$\Pi(k) = \tilde{\Pi}(k) - \frac{\zeta(k)}{2\mathcal{O}_2(k)}\mathcal{O}_3(k). \tag{3.4.4}$$

This then yields:

$$P[\zeta] = \int \mathcal{D}\tilde{\Pi} \exp\{-\frac{1}{4\pi^2}\int dk k^2[\zeta\mathcal{O}_1\zeta - \frac{1}{4}\zeta\frac{\mathcal{O}_3^2}{\mathcal{O}_2}\zeta + \tilde{\Pi}\mathcal{O}_2\tilde{\Pi}]\}. \tag{3.4.5}$$

The first two terms in the exponential can be taken outside of the path integral, and the resulting path integral is a standard Gaussian path integral which yields a constant factor related to the determinant of $\mathcal{O}_2$ that will only contribute to the normalization. Because we will fix that later we neglect it here, yielding:

$$P[\zeta] \propto \exp\{-\frac{1}{4\pi^2}\int dk k^2\zeta(k)\mathcal{O}(k)\zeta(k)\} \tag{3.4.6}$$

where

$$\mathcal{O}(k) = (\mathcal{O}_1(k) - \frac{\mathcal{O}_3^2(k)}{4\mathcal{O}_2(k)}). \tag{3.4.7}$$

Once again, this expression does not just depend on the power spectrum, but also on the $\zeta - \Pi$ and $\Pi - \Pi$ correlators.

Usually, the momentum correlators are neglected. If inflation ends with a period of slow roll, this is justified because in that case $\dot{\zeta} \approx 0$ for the modes crossing the horizon. However, we have already noted that slow roll inflation only cannot produce

PBHs. For any theory with enhancement of the fluctuations on small scales, these momentum correlators might be significant, and therefore have to be taken into account.

3.5 Connecting to correlation functions

In appendix IV it is shown that in terms of the correlation functions we have:

$$\mathcal{O}(k,t) = \frac{\Delta^2(\vec{k},t)}{2\langle\zeta(\vec{k},t)\zeta^*(\vec{k},t)\rangle}, \tag{3.5.1}$$

where Δ^2 is the Gaussian invariant defined in real space by: [40]

$$\Delta^2(\vec{x},\vec{y};t) = \langle\zeta(\vec{x})\zeta(\vec{y})\rangle\langle\Pi(\vec{x})\Pi(\vec{y})\rangle - \frac{1}{4}\langle\{\zeta(\vec{x}),\Pi(\vec{y})\}\rangle^2. \tag{3.5.2}$$

Because of the homogeneity and isotropy, these correlation functions only depend on $k = |\vec{k}|$ in Fourier space. Furthermore, $\mathcal{O}$ depends not only on the power spectrum, but also on the momentum-field and momentum-momentum correlation functions. We have that $\Delta^2 \geq 1$, with equality for a pure state, so the definition can also be seen as a version of the uncertainty principle for general Gaussian states [40]. In the pure case, $\mathcal{O}$ only depends on the power spectrum as:

$$\mathcal{O}(k,t) = \frac{k^3}{4\pi^2\mathcal{P}_\zeta(k,t)}. \tag{3.5.3}$$

So assuming both a pure state and no criteria on the momentum perturbations the probability for ζ reduces to:

$$P[\zeta;t] \propto \exp\{-\frac{1}{8\pi^2}\int dk k^2\zeta(k,t)k^3\mathcal{P}_\zeta(k,t)^{-1}\zeta(k,t)\}. \tag{3.5.4}$$

However, both of these assumptions might not be applicable. The Gaussian invariant Δ^2 is intimately related to the amount of entropy and decoherence in the state. As the name suggests, it is invariant in a quadratic theory like the one we study here, but in the general evolution of the universe it is not, and it can increase, signifying the decoherence of the state. A preliminary result of [41] suggests that even in presence of small interactions, Δ^2 can rapidly grow during inflation. To investigate this fully is beyond the scope of this thesis however, and we will stick to the case of $\Delta^2 = 1$.

3.6 The compaction function in terms of the curvature perturbation

In this section, we relate ζ to the compaction function, so we can transform the probability we just described into one for $\mathcal{C}$. Recall that the definition of the

compaction function is:

$$\mathcal{C} = \frac{2G\delta M(r,t)}{R(r,t)}. \tag{3.6.1}$$

Where G is Newtons constant, $\delta M(r,t)$ is the mass excess in a spherical region with comoving radius r and R is the physical radius $R(r,t) = a(t)re^{\zeta(r)}$.

The mass excess can be found by integrating over the density perturbation inside the sphere:

$$\delta M(r,t) = 4\pi \int_0^{R(r,t)} \delta\rho(R',t)R'^2 dR'. \tag{3.6.2}$$

Making a transformation to $r = Re^{-\zeta(r)}/a$ yields:

$$\delta M(r,t) = 4\pi a^3 \int_0^r dr'(1 + r'\partial_r\zeta(r'))e^{\zeta(r')}r'^2\delta\rho(r') \tag{3.6.3}$$

Where $\delta\rho(r,t) = \rho(r,t) - \bar{\rho}_b(t)$ is the density contrast with the background energy density $\rho_b(t) = 3M_p^2H^2(t)$.
From the Einstein equation we have the relativistic Poisson equation for $\delta\rho$ [22]:

$$\delta\rho(r,t) \approx -\frac{24M_p^2}{9a^2(t)}e^{-5/2\zeta(r)}\nabla^2 e^{\zeta(r)/2}. \tag{3.6.4}$$

Hence, to first order in ζ, which suffices for this thesis because we only look at the second order action for ζ which only has quadratic terms, we have:

$$\delta M(r) = 4\pi a^3 \int_0^r dr' r'^2 \delta\rho(r'), \tag{3.6.5}$$

where we neglect any angular dependence of the perturbation: we assume that it is spherically symmetric. This amounts to decomposing the perturbation into spherical harmonics and only looking at the zeroth-order term: to take nonsphericity into account we would have to look at higher order terms.
We ignore the time-dependence of all functions from now on in this section to make the expressions more compact. $\mathcal{C}$ is a function of the radius of the overdensity that might collapse to form a PBH. This means that we cannot simply treat $\mathcal{C}(r,t)$ as a function of a point in space only dependent on the radial coordinate: we must treat it as an integrated quantity that has no more dependence on angles: it described the properties of a sphere with radius r. To make sense of how to Fourier transform $\mathcal{C}$, it is still convenient to introduce a non-integrated $\mathcal{C}(\vec{x})$ as a function of position such that:

$$\mathcal{C}(r) = \int d\Omega \mathcal{C}(\vec{x}). \tag{3.6.6}$$

Where the norm of $\vec{x}$ is r. Then $\mathcal{C}(\vec{x})$ can be Fourier transformed using the usual technique. In particular, we have:

$$\mathcal{C}(x) = \int d\Omega_x \int \frac{d\vec{k}}{(2\pi)^3} e^{i\vec{k}\cdot\vec{x}} . \mathcal{C}(\vec{k}) \tag{3.6.7}$$

Now the only dependence on the angles of $\vec{x}$ is in the exponential, and this can be integrated out, yielding:

$$\mathcal{C}(r) = 4\pi \int \frac{d\vec{k}}{(2\pi)^3} \frac{\sin(|\vec{k}|r)}{|\vec{k}|r} \mathcal{C}(\vec{k}). \tag{3.6.8}$$

The only angular dependence is now in the unknown dependence of $\mathcal{C}(\vec{k})$ on the angles. This means we can formulate the fourier transform in terms of another integrated quantity, namely:

$$\mathcal{C}(k) = \int d\Omega_k \mathcal{C}(\vec{k}). \tag{3.6.9}$$

Where from now on we denote $|\vec{k}| = k$, and likewise for other vectors. We get:

$$\mathcal{C}(r) = \frac{1}{2\pi^2 r} \int_0^\infty dk k \sin(kr) \mathcal{C}(k). \tag{3.6.10}$$

Working out the inverse transformation in the same way yields:

$$\mathcal{C}(k) = \frac{4\pi}{k} \int_0^\infty dr r \sin(kr) \mathcal{C}(r). \tag{3.6.11}$$

These are the right definition for the Fourier transform of any quantity only dependent on the radius, and we will use them throughout this thesis. From this, we can start to express $\rho(\vec{k})$ in terms of $\mathcal{C}$ to in the end connect the results for ζ to the probability of PBH formation.
We have:

$$\mathcal{C}(k) = 4\pi \int_0^\infty dr \frac{r}{k} \sin(kr) \mathcal{C}(r) \tag{3.6.12}$$

$$= 8\pi G \int_0^\infty dr \sin(kr) \frac{r\delta M(r)}{k a e^{\zeta(r)} r} \tag{3.6.13}$$

$$= 32\pi^2 G a^2 \int_0^\infty dr \frac{\sin(kr)}{k} \int_0^r \delta\rho(r') r'^2 dr' \tag{3.6.14}$$

to first order in $\delta\rho(r)$. Now $\delta\rho(r)$ is in fact not an integrated quantity: the density perturbation is defined for every point in space, so it is in fact a function of r, θ and ϕ that has trivial dependence on the angles because we look at a spherically symmetric perturbation. This means we can reinstate the integral over the angles,

which yields a factor of $1/4\pi$, so that we get an integral over a 3D function to make the process of Fourier transforming $\delta\rho$ more transparent. This yields:

$$= 32\pi^2 G a^2 \int_0^\infty dr \frac{\sin(kr)}{k} \int d\vec{x}\delta\rho(\vec{x})\theta(r - |\vec{x}|). \tag{3.6.15}$$

Where we have implemented the boundary at a radius of r as a theta function. Next, we Fourier transform $\rho(\vec{x})$ and $\theta(r - |\vec{x}|)$, which yields:

$$\mathcal{C}(k) = \frac{a^2}{2\pi^4} G \int_0^\infty dr \frac{\sin(kr)}{k} \int d\vec{x} d\vec{k'} d\vec{k''} \delta\rho(\vec{k'})\tilde{\theta}(\vec{k''}) e^{i\vec{x}\cdot(\vec{k'}+\vec{k''})}. \tag{3.6.16}$$

Where we have for $\tilde{\theta}$:

$$\tilde{\theta}(\vec{k''}) = \int d\vec{x'}\theta(r - |\vec{x'}|)e^{-i\vec{x'}\cdot\vec{k'}}. \tag{3.6.17}$$

Integrating over the angles and putting the theta function into the integration boundary for the radial integral yields:

$$\tilde{\theta}(\vec{k''}) = 4\pi \int_0^r dr' r'^2 \frac{\sin(r'|\vec{k''}|)}{r'|\vec{k''}|}. \tag{3.6.18}$$

Then the integral over the radius can be performed:

$$\tilde{\theta}(\vec{k''}) = \frac{4\pi}{|\vec{k''}|^3}(\sin(|\vec{k''}|r) - |\vec{k''}|r\cos(|\vec{k''}|r)). \tag{3.6.19}$$

Note that $\tilde{\theta}$ only depends on the norm of $\vec{k''}$, not the angles.
Now in the expression for $\mathcal{C}(k)$ we can perform the integral over $\vec{x}$, which yields a delta function of $\delta^3(\vec{k''} + \vec{k})$. Using this the integral over $\vec{k''}$ can be evaluated. This yields:

$$\mathcal{C}(k) = \frac{4Ga^2}{\pi} \int_0^\infty dr \frac{\sin(kr)}{k} \int d\vec{K'}\delta\rho(\vec{k'})\tilde{\theta}(-\vec{k'}) \tag{3.6.20}$$

$$\mathcal{C}(k) = \frac{16Ga^2}{k} \int d\vec{k'} \frac{\delta\rho(\vec{k'})}{k'^3} \int_0^\infty dr \sin(kr)(\sin(k'r) - k'r\cos(k'r)). \tag{3.6.21}$$

The integrals over r do not converge at this point, but we can regulate them by adding a term of $e^{-\epsilon r}$ to the integrand, with $\epsilon > 0$ infinitesimal. Using this, it is derived in appendix III that:

$$\int_0^\infty dr \sin(kr)\sin(k'r) = \frac{\pi}{2}[\delta(k + k') - \delta(k - k')] \tag{3.6.22}$$

and

$$k' \int_0^\infty dr r \sin(kr)\cos(k'r) = -\frac{\pi k'}{2}\frac{\partial}{\partial k}[\delta(k+k') + \delta(k-k')]. \tag{3.6.23}$$

Because k and k' are positive, the delta functions with a plus do not contribute, so we have:

$$\mathcal{C}(k) = \frac{2Ga^2}{k}\int d\vec{k'}\frac{\delta\rho(\vec{k'})}{k'^3}(1 + k'\frac{\partial}{\partial k})\delta(k-k'). \tag{3.6.24}$$

Now as we have assumed that the perturbation is spherically symmetric, $\delta\rho(\vec{x})$ only depends on the norm of $\vec{x}$, and therefore $\delta\rho(\vec{k})$ also has no dependence on the angular integrals. Therefore, those integrals are trivial, and we find:

$$\mathcal{C}(k) = \frac{8\pi Ga^2}{k}\int_0^\infty dk'\delta\rho(k')(\frac{1}{k'} + \frac{\partial}{\partial k})\delta(k-k'). \tag{3.6.25}$$

We can take the derivative over k out of the integral now, as nothing else inside depends on it. Then we can evaluate the integral using the delta function, yielding:

$$\mathcal{C}(k) = \frac{8\pi Ga^2}{k}(\frac{1}{k} + \frac{\partial}{\partial k})\delta\rho(k). \tag{3.6.26}$$

Which can be rewritten as:

$$\frac{\partial}{\partial k}(k\delta\rho(k)) = \frac{k^2}{8\pi Ga^2}\mathcal{C}(k). \tag{3.6.27}$$

Integrating 1both sides yields:

$$k\delta\rho(k) = k^2\delta\rho(k)|_{k=0} + \frac{1}{8\pi Ga^2}\int_0^k dk'k'^2\mathcal{C}(k'). \tag{3.6.28}$$

Now we have that $\delta\rho$ should not diverge when going to very large scales, since the density perturbation is known to be small at large scales and this would be unphysical, so $\delta\rho(k)k^2$ goes to zero as $k \to 0$. This means we get:

$$\delta\rho(k) = \frac{1}{8\pi Ga^2 k}\int_0^k dk'k'^2\mathcal{C}(k'). \tag{3.6.29}$$

$\delta\rho(k)$ can then be expressed in terms of $\zeta(k)$, using the relativistic Poisson equation to first order in ζ:

$$\delta\rho(r,t) = -\frac{4M_p^2}{3a^2(t)}\nabla^2\zeta(r). \tag{3.6.30}$$

Now we can Fourier transform this expression, which yields:

$$\delta\rho(k) = -\frac{4M_p^2}{3a^2}\int d\vec{x}e^{-i\vec{x}\cdot\vec{k}}\nabla^2\zeta(r). \tag{3.6.31}$$

$$\delta\rho(k) = \frac{4M_p^2k^2}{3a^2}\int d\vec{x}\zeta(r)e^{-i\vec{x}\cdot\vec{(k)}} = \frac{4M_p^2k^2}{3}\zeta(k). \tag{3.6.32}$$

So in the end, we find the relation:

$$\zeta(k) = \frac{3a^2}{4M_p^2k^2}\delta\rho(k) \tag{3.6.33}$$

$$\zeta(k) = \frac{3}{4k^3}\int_0^k dk'k'^2\mathcal{C}(k'). \tag{3.6.34}$$

This can then be substituted into the expressions found for $\mathcal{C}$ in terms of ζ to get the probability density for $\mathcal{C}$. This nonlocal relation between the two has a field-independent Jacobian, so it can be absorbed in the normalization. This yields, reinstating the time-dependence:

$$P[\mathcal{C},t] \propto \exp\{-\frac{1}{4\pi^2}\int dkk^2\frac{9\mathcal{O}(k,t)}{16k^6}|\int_0^k dqq^2\mathcal{C}(q,t)|^2\}, \tag{3.6.35}$$

now we can use that $\mathcal{C}(r)$ is real and only depends on the radial coordinate, and therefore its Fourier transform $\mathcal{C}(q)$ is also real as noted in section 3.5. This means we can write:

$$\propto \exp\{-\frac{1}{2}\int dqdq'\mathcal{C}(q,t)K(q,q';t)\mathcal{C}(q',t)\}, \tag{3.6.36}$$

where we have defined the kernel:

$$K(q,q';t) = \frac{9}{32\pi^2}\int_0^\infty dk\frac{\mathcal{O}(k,t)}{k^4}\theta(k-q)\theta(k-q')q^2q'^2. \tag{3.6.37}$$

This is then finally normalised to be a proper probability: we require

$$\int \mathcal{D}\mathcal{C}P[\mathcal{C}] = 1. \tag{3.6.38}$$

From which it is found by a standard Gaussian path integral that:

$$P[\mathcal{C};t] = \sqrt{\det(K)}\exp\{-\frac{1}{2}\int dqdq'\mathcal{C}(q,t)K(q,q';t).\mathcal{C}(q',t)\} \tag{3.6.39}$$

Which is the probability distribution for $\mathcal{C}$ we set out to find in this chapter: it turns out to be Gaussian, but with a complicated kernel. We will not need to calculate or regulate the functional determinant of this kernel explicitly: it will drop out again when we calculate the formation probability of PBHs in the next chapter.

Chapter 4

Evaluating the probability

In this chapter, the probability distribution for $\mathcal{C}$ that was found in the last chapter is used to determine the PBH spectrum for any given theory of inflation. For this, we have to implement the criteria for PBH formation. The way we implement Musco's first criterion, which states that value of the compaction function has to be greater than some critical value, is by adding in a step function to the path integral.

$$P(r,t)_{PBH} = \int \mathcal{D}\mathcal{C}P[\mathcal{C};t]\delta(\partial_r \mathcal{C}(r,t))\theta(\mathcal{C}(r,t) - C_{crit}) \tag{4.0.1}$$

In this way, all of the profiles for which $\mathcal{C}(r,t)$ is not large enough are projected out, and we are left with the fraction of profiles that forms a PBH, weighted with their probability. This formula therefore describes the probability for a given sphere of radius r at time t that there is a density fluctuation sufficiently large to surpass the critical value and collapse into a PBH.

We have not yet been able to implement Musco's second criterion, that fixes the scale of formation to be at the maximum of the compaction function. We expect that ignoring this criterion will not change the mass spectrum very much, because PBHs form from very rare perturbations. A radius at a given time where the compaction function is large enough but not at its maximum will still form a PBH, but just with a different radius. Because it only rarely happens that $\mathcal{C} > \mathcal{C}_c$, any such $\mathcal{C}$ will never be far away from $\mathcal{C}_c$. Therefore, the radius at which the criterion is fulfilled is never far away from the radius of the region that will collapse. Because the radius will directly determine the mass of the PBH, the mass spectrum of PBHs will only shift slightly.

4.1 Evaluating the path integral

In this section, we work out the calculation of the probability by this path integral. The step function can be written as follows:

$$\theta(\mathcal{C}(r,t)-\mathcal{C}_{crit}) = \frac{1}{2\pi i}\int \frac{dx}{x-i\epsilon} e^{ix(\mathcal{C}(r,t)-\mathcal{C}_{crit})} \tag{4.1.1}$$

$$= \frac{1}{2\pi i}\int \frac{dx}{x-i\epsilon} \exp\{-ix\mathcal{C}_{crit} + \frac{ix}{2\pi^2 r}\int_0^\infty dqq\sin(qr)\mathcal{C}(q)\}, \tag{4.1.2}$$

which yields for the total path integral:

$$P(r,t) = \frac{\sqrt{\det(K)}}{2\pi i}\int \mathcal{DC}\int_{-\infty}^{\infty}\frac{dx}{x-i\epsilon}\exp\{-ix\mathcal{C}_{crit} \tag{4.1.3}$$

$$+\frac{ix}{2\pi^2 r}\int dqq\sin(qr)\mathcal{C}(q) - \frac{1}{2}\int dqdq'\mathcal{C}(q,t)K(q,q';t)\mathcal{C}(q',t)\}. \tag{4.1.4}$$

Now we can complete the square to perform the integral over $\mathcal{C}$ by transforming:

$$\mathcal{C}(q,t) = \mathcal{C}(\tilde{q},t) + \frac{i}{2\pi^2 r}\int dq' K^{-1}(q,q';t)q'x\sin(q'r). \tag{4.1.5}$$

Where K^{-1} is defined by:

$$\int dk K(q,k;t)K^{-1}(k,q';t) = \delta(q-q'). \tag{4.1.6}$$

In appendix II it is shown that an inverse for the kernel is given by:

$$K^{-1}(q,q';t) = -\int_0^\infty dk \frac{16\pi^2 k^4}{9\mathcal{O}(k,t)q^2 q'^2}\partial_q\delta(q-k)\partial_k\delta(q'-k) + (q\leftrightarrow q'). \tag{4.1.7}$$

This yields for the probability:

$$P(r,t) = \frac{\sqrt{\det(K)}}{2\pi i}\int \frac{dxe^{-ix\mathcal{C}_{crit}}}{x-i\epsilon}\int \mathcal{DC}\exp\{-\frac{1}{2}\int dqdq'\mathcal{C}(q,t)K(q,q';t)\mathcal{C}^*(q',t)$$

$$-\frac{1}{2}\int dqdq'\frac{1}{2\pi^2 r}qx\sin(qr)K^{-1}(q,q';t)\frac{1}{2\pi^2 r}q'x\sin(q'r)\}. \tag{4.1.8}$$

The path integral over $\mathcal{C}$ is a standard Gaussian path integral, yielding:

$$P(r,t) = \frac{1}{2\pi i}\int \frac{dx e^{-ix\mathcal{C}_{crit}}}{x - i\epsilon} \exp\{-\frac{1}{2}\int dq dq' \frac{qx\sin(qr)}{2\pi^2 r} K^{-1}(q,q';t)\frac{qx\sin(qr)}{2\pi^2 r}\} \tag{4.1.9}$$

$$= \frac{1}{2\pi i}\int \frac{dx e^{-ix\mathcal{C}_{crit}}}{x - i\epsilon} \exp\{-\frac{x^2}{8\pi^4 r^2}\int dq dq' qq' \sin(qr)\sin(q'r)K^{-1}(q,q';t)\}. \tag{4.1.10}$$

From this we find:

$$P(r,t) = \frac{1}{2\pi i}\int \frac{dx e^{-ix\mathcal{C}_{crit}}}{x - i\epsilon} \exp\{-x^2 g(r,t)\} \tag{4.1.11}$$

with

$$g(r,t) = \frac{1}{8\pi^4 r^2}\int dq dq' qq' \sin(qr)\sin(q'r)K^{-1}(q,q';t). \tag{4.1.12}$$

This function $g(r,t)$ gives a dimensionless number depending on r and t which contains the information about the power spectrum of the theory via the inverse kernel.

We then need the following integral, which is proven in appendix I:

$$\int_{-\infty}^{\infty} \frac{dx}{x - i\epsilon} e^{-ix\mathcal{C}_c - g(r)x^2} = i\pi \ \mathrm{erfc}(\frac{\mathcal{C}_c}{2\sqrt{g(r)}}). \tag{4.1.13}$$

Applying this yields the following expression for the formation probability of a PBH:

$$P(r,t) = \frac{1}{2}\mathrm{erfc}(\frac{\mathcal{C}_c}{2\sqrt{g(r,t)}}). \tag{4.1.14}$$

This is one of the main results of this thesis: the probability of a given sphere of radius r at time t to collapse and form a PBH. In this formula the complimentary error function behaviour of the naive equation 1.4.13 for the abundance is recovered, but now with a highly nontrivial, well-defined function $g(r,t)$ that depends on $K^{-1}(q,q';t)$, which again very nontrivially depends on the power spectrum. To determine the probability from a given power spectrum, one needs to calculate:

$$g(r,t) = -\frac{1}{4\pi^2 r^2}\int_0^{\infty} dq dq' dk \frac{16k^4}{9\mathcal{O}(k,t)q^2 q'^2}\partial_q\delta(q-k)\partial_k\delta(q'-k)qq'\sin(qr)\sin(q'r) \tag{4.1.15}$$

where we have used that integral is symmetric in q and q'. This can be partially integrated twice to yield:

$$= -\frac{4}{9\pi^2 r^2}\int_0^\infty dq dq' dk \frac{\partial}{\partial k}[\frac{k^4}{\mathcal{O}(k,t)}]\frac{\partial}{\partial q}[\frac{\sin(qr)}{q}]\frac{\sin(q'r)}{q'}\delta(q-k)\delta(q'-k) \quad (4.1.16)$$

$$= -\frac{4}{9\pi^2 r^2}\int_0^\infty dk \frac{kr\cos(kr)-\sin(kr)}{k^2}\frac{\sin(kr)}{k}\frac{\partial}{\partial k}[\frac{k^4}{\mathcal{O}(k,t)}] \quad (4.1.17)$$

with $\mathcal{O}(k,t)$ given by:

$$\mathcal{O}(k,t) = \frac{k^3}{4\pi^2\mathcal{P}_\zeta(k,t)}. \quad (4.1.18)$$

In this way, the probability is uniquely defined from the power spectrum, without having made any choice for a window function and having taken the full field theory behaviour into account.

4.2 The probability for the enhanced power spectrum

At this point, we have assumed that perturbations can only form PBHs at scales smaller than or equal to the Hubble radius. There is no reason why the probability should be 0 for perturbations on super-Hubble scales however. We will still ignore these cases as it is not clear to us how large super-Hubble perturbations will back-react to the background. It is imaginable that a large enough perturbation might stop inflation from proceeding in a region, invalidating the background evolution of the scale factor that we assume and for instance form a super-Hubble black hole within which the expansion might continue. A full treatment of the effect of this backreaction on the stress-energy tensor is beyond the scope of this thesis, but might be necessary to interpret the results and is certainly interesting in itself. This means however, that we will only consider PBH formation at the scale of the Hubble radius.

As is shown in section 2.6 ,the compaction function for perturbations that cross the horizon in the radiation era decreases quickly after Hubble crossing, so it is a good approximation to only check if a perturbation is large enough to form a PBH at the Hubble radius. This means only the power spectrum at horizon crossing is necessary as the input for the calculation, and as g only depends on time through the power spectrum, this makes it a function of radius only. As mentioned in chapter 2, we can take the following form that is enhanced at small scales:

$$\mathcal{P}_\zeta(k) = \mathcal{P}_0(\frac{k}{k_*})^{n_s-1}(1+Af(k-k_0)). \quad (4.2.1)$$

Here k_* is a reference scale, P_0 the amplitude of the background fluctuations, k_0 the scale above which the enhancement kicks in, $f(x)$ a function that switches between 0 and 1 around $x=0$ and A the magnitude of the enhancement. This is in reasonable

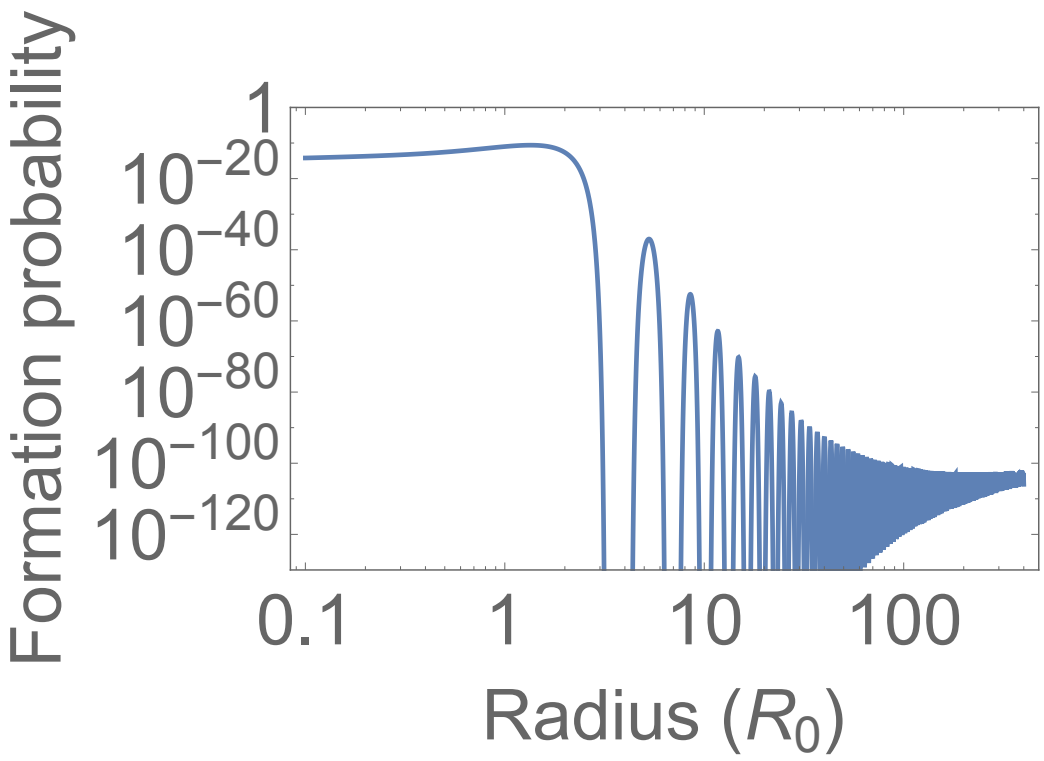

Figure 4.1: The probability of a spherical region of the universe to collapse into a PBH as a function of its physical radius. The chosen parameters are $\mathcal{P}_0 = 2 * 10^{-4}$, $A = 10$, $K_0 = 1$ and $n_s = 0.96$. The scale of the radius is given by $R_0 = \frac{2\pi}{K_0}$.

agreement with the exact results for the model seen in chapter 2 for scales not too far from the critical scale. At first we will use a step function for the switching function, which actually yields an exact result. This will be compared with numerical results from more physical, continuous functions later.

This means that we have:

$$\frac{1}{\mathcal{O}(k,t)} = 4\pi^2 \mathcal{P}_0 k_*^{n_s-1} k^{n_s-4}(1 + A\theta(k - k_c)). \tag{4.2.2}$$

Filling this into the formula for $g(r)$ gives:

$$g(r) = -\frac{16}{9r^2}\int_0^\infty dq dq' dk \frac{k^4}{q^2 q'^2}\partial_q\delta(q-k)\partial_k\delta(q'-k)\mathcal{P}_0^* k^{n_s-4}(1+A\theta(k-k_c))q\sin(qr)q'\sin(q'r). \tag{4.2.3}$$

It turns out this equation can be solved exactly, which yields:

$$g(r,t) = \frac{2^{-3-n_s}\mathcal{P}_0 r^{-2-n_s}}{k_0^3(n_s-3)\pi^4}(-2^{n_s}An_s(k_0r)^{2+n_s}{}_2F_1(\frac{n_s-1}{2},\frac{3}{2},\frac{n_s+1}{2},-k_0^2r^2)$$
$$-2(1+A)k_0^3r^3n_s(3-4n_s+n_s^2)\Gamma(n_s-3)\sin(n_s\pi/2)$$
$$+2^{n_s}A(k_0r)^{n_s}\sin(k_0r)(k_0r(n_s-3)\cos(k_0r)+3\sin(k_0r))) \quad (4.2.4)$$
$$(4.2.5)$$

where ${}_2F_1(a,b,c,x)$ is a hypergeometric function. This is already a rather complicated answer for the very simplest case, so usually the integrals defining g have to be performed numerically. What we see here is that the radius always enters as either k_0r or k_*r, where k_0 and k_* are the comoving switching scale and reference scale from the slow roll power spectrum respectively. This is true in general, as these are the only scales in the problem. As input for these however, we do not want to define a comoving critical scale, but a physical scale $K_0 = \frac{k}{a}$ that does not evolve with the expansion of the universe. Hence, r only enters as ar or the physical radius, which is very useful when relating it to the mass of the PBH formed.

In figure 4.1, the probability that a region will collapse to form a PBH when its radius crosses the Hubble radius is plotted against the physical radius of the region. In this plot, we clearly see that there is a switching behaviour, with the probability being large for small radii and vice versa as expected. More PBHs form at small radii, when the power spectrum is enhanced, and below the critical radius the power spectrum become approximately scale invariant again. The scale of the oscillations is set by K_0, and as we will see later they arise depending on the steepness of the switch. It must be noted here that we have not chosen a realistic value for P_0, the slow roll background amplitude. In our universe, we have $P_0 \sim 10^{-9}$, so whereas the probability only goes to 10^{-100} in this plot on large scales, for our universe Mathematica gives an absurdly small $10^{-25000000}$, although we wonder whether numerics can be trusted for these minuscule numbers. This makes it very clear nevertheless that no PBHs will form at all if there is only slow roll inflation.

4.3 Towards the PBH mass spectrum

We have up to now calculated the quantity $P(r,t)$, which we took to be time-independent because we evaluated it only at Hubble crossing, yielding the function $P(R)$, the probability of a sphere of physical radius $R = a(t)r$ to collapse into a PBH when this is the physical Hubble radius $R = \frac{1}{H}$. To relate this to the mass spectrum of PBHs at formation $\beta(M)$, we need to know what the relation between the radius of a collapsing sphere and the mass of the PBH that will form is. This mass can be approximated by the following formula:[2]

$$M_{PBH} = \gamma M_H. \tag{4.3.1}$$

Where M_H is the background mass of the Hubble volume that collapses and γ is a numerical parameter that depends on the details of the collapse and that simulations put around 0.4. The mass of the Hubble volume can be directly calculated from the radius by:

$$M_H = \frac{4\pi}{3} R^3 \rho = 4\pi R M_p^2 \tag{4.3.2}$$

where we have used the first Friedmann equation 1.1.5 for the background density. Using these two equations, the radius of the region that will collapse is related to the PBH mass by:

$$R = \frac{M_{PBH}}{4\pi\gamma M_p^2}. \tag{4.3.3}$$

Now the number density of PBHs of mass M at formation is the probability that a region which, if it collapses, will form a PBH of mass M, will actually collapse. Hence, we have an expression for $\beta(M)$ in terms of P, given by:

$$\beta(M) = P(\frac{M_{PBH}}{4\pi\gamma M_p^2}) \tag{4.3.4}$$

which we can now calculate for any given Gaussian theory of inflation as long as we know its correlators or density matrix. The mass formula we used is however just an approximation: for a full description the mass of the PBH that forms has to be found from the theory of critical collapse, which gives the following:

$$M_{PBH} = k M_H \left(\delta - \delta_c\right)^{\gamma_2} \tag{4.3.5}$$

where δ is the overdensity integrated over the collapsing volume, γ_2 is a critical exponent and k a constant[2]. This formula means that PBHs with a wide range of masses can form from a specific radius, making it more difficult to calculate β from the probability. This might be possible to solve in our framework by introducing this relation already inside the path integral, and writing the factor of δ that appears in terms of $\mathcal{C}$. However, this is beyond the scope of this thesis.

Another factor that might change the relation between β and P is accretion. If a large amount of matter falls into a PBH after formation, it will be much heavier. This can be thought of as an effective increase in γ [2], and this is not a very big problem for describing the general behaviour of PBH formation because it only enters in the equation for β multiplied with K_0, and is hence completely degenerate with it, provided the spectrum $\beta(M)$ is not very broad. As K_0 is a model-dependent parameter that we are completely free to choose, only a nontrivial scale-dependence

of the accretion rate might give qualitatively different results. For quantitative investigations into PBH formation from a given theory of inflation however, this effect might have to be taken into account.
We can now apply this and study the dependence on the switching profile by looking at a more realistic power spectrum, namely:

$$\mathcal{P}_\zeta(k) = \mathcal{P}_{SR}(k)\,(1 + A\tanh(s(K - K_0)) \tag{4.3.6}$$

where the parameter s determines the steepness of the switch. The numerical results for this power spectrum are shown in figure 4.2. From this it is clear that the oscillations are caused by the quick transition between low and high power, and that smoothing out this transition makes them dampen faster and eventually disappear.

Another thing to note is that the value of β at small scales, which directly translates to the number of PBHs in our universe today, is highly model-dependent. The probability at small scales is exponentially sensitive to the value of A assumed in the model, so any theory predicting the right number of PBHs to form dark matter today must be extremely fine-tuned or have some mechanism that stabilizes the enhancement at precisely the right value. The formation probability is plotted against M for a step function enhancement in figure 4.3, where it can be seen that it goes to 1/2 for large values of A. This makes sense, as our model makes no difference between over- and underdensities, and even if the fluctuations are large enough that any overdensity will collapse to a PBH, there might just as well be an equally big underdensity. Of course, the symmetry between over- and underdensities will fail at much lower fluctuation sizes, as will many other assumptions we made along the way, but it is nevertheless a good reality check.

Summing up, in this chapter we have shown how to calculate the probability of PBH formation and the PBH mass spectrum from the probability distribution of ζ. We ignored Musco's second constraint, arguing that its effect would be small as PBHs are rare, and got reasonable results that reduce to the erfc-behaviour found in the naive calculation, but give a specific prescription for the smoothing and can take significant momentum correlators into account.

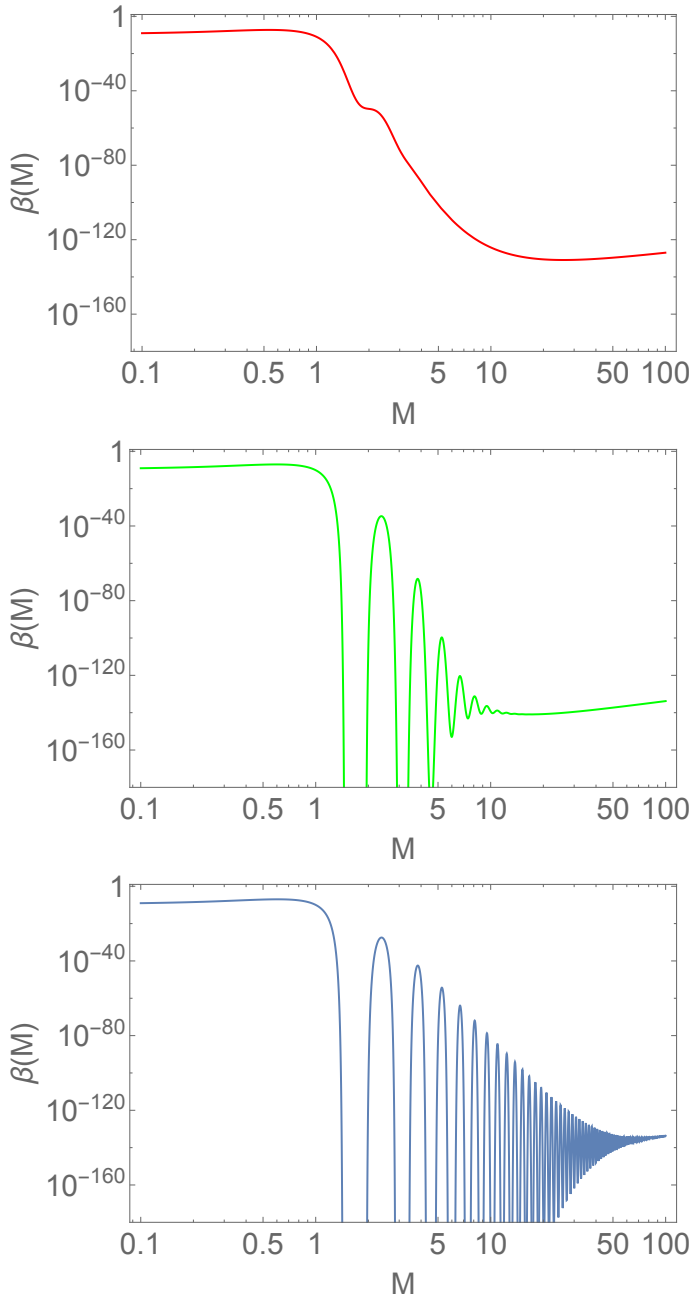

Figure 4.2: The PBH spectrum at formation $\beta(M)$ for a hyperbolic tangent enhancement function as in equation 4.3.6 with different steepness s: $s = 2.5$ in red, $s = 5$ in green and $s = 10$ in blue. The other parameters are the same as in figure 4.1, and we have set $\gamma = 0.4$. The mass is given in terms of the mass corresponding to the collapse of a region with size $\frac{2\pi}{K_0}$, $M_0 = \frac{\pi\gamma}{K_0}$. Note that the last figure resembles the exact result shown in figure 4.1, so in the limit $s \to \infty$ the behaviour of the step function is recovered.

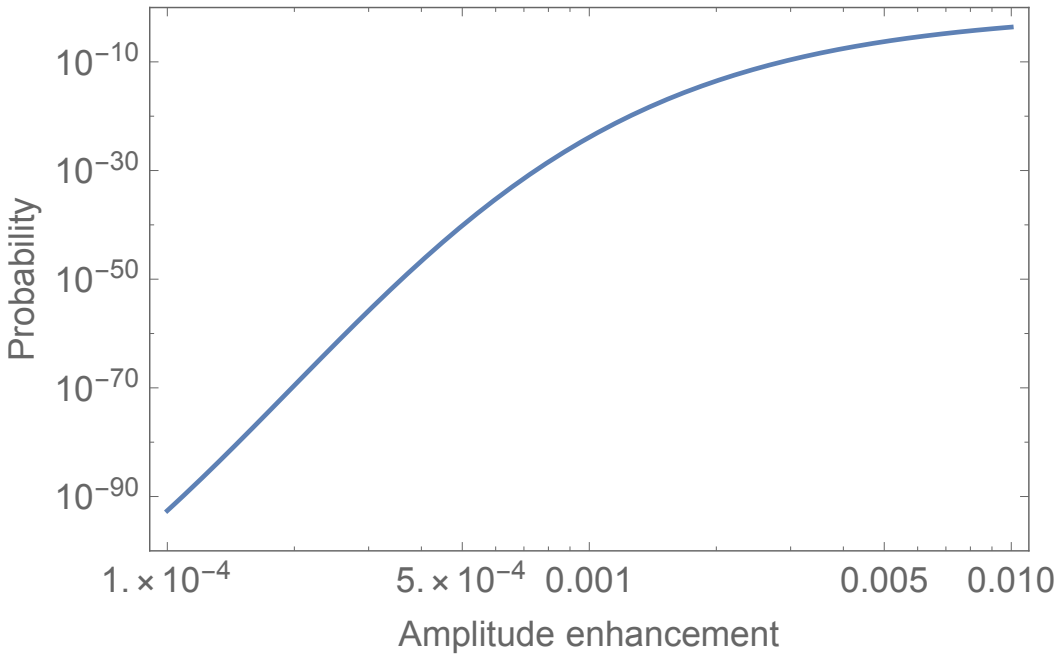

(a) The formation probability of a PBH at $R = 0.2R_0$, with the same parameters otherwise as in figure 4.1, plotted on a log scale against the relative enhancement of the amplitude $A\mathcal{P}_0$.

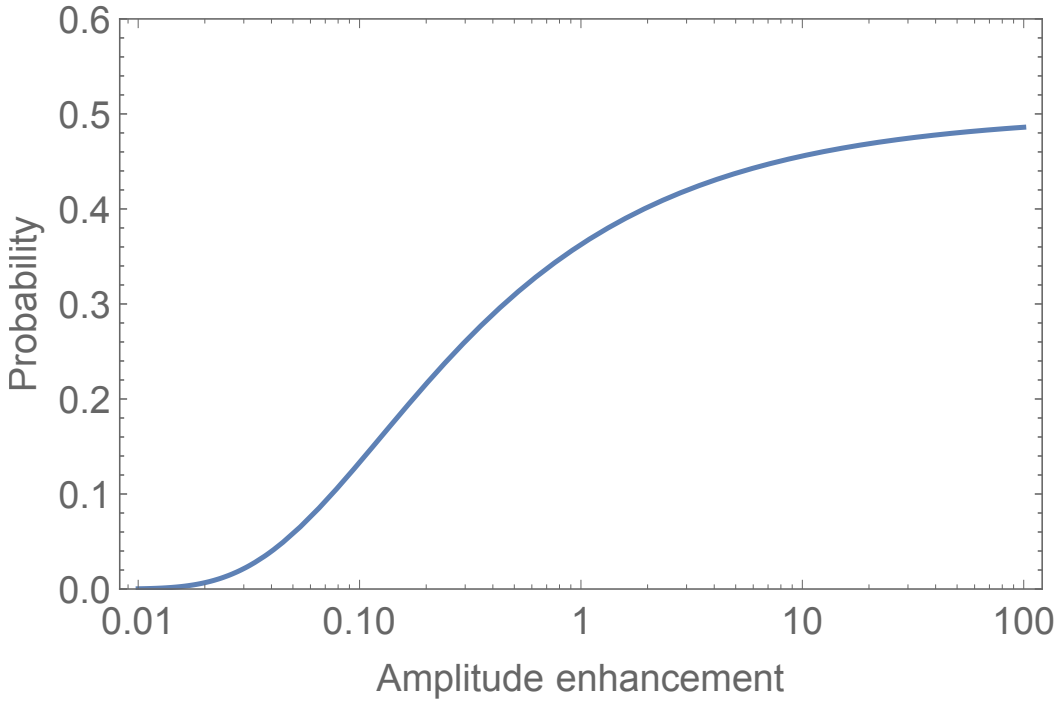

(b) The formation probability of a PBH at $R = 0.2R_0$, with the same parameters as in the above figure, but now plotted on a linear scale for large relative amplitude enhancements. From this plot, it can be seen that the formation probability approaches $\frac{1}{2}$ as the enhancement becomes very large.

Figure 4.3

Chapter 5

Discussion and Conclusion

In this thesis, we have introduced a framework in which the probability of PBH formation can be calculated directly from the density matrix of any state produced by inflation. This results in an expression that reduces to the complimentary error function description seen before, but extended and with a specific, well-defined way to relate the local perturbations to the non-local collapse probability. These probabilities for power spectra enhanced at small scales agree with our expectations, but we are aware that number of assumptions have been made in coming to our results. These are also main motivations for future work, since many of them might be incorporated into this framework.

Firstly, we have only worked to leading order in ζ many times, whereas ζ is expected to large when forming PBHs. This is not a problem in our derivation of the slow roll power spectrum, since we take general power spectra as input for our calculation and do not care how they were calculated. The place where this poses a problem is in the relation between ζ and $\delta\rho$, which we used to write ζ in terms of $\mathcal{C}$. Another factor is that the physical radius will also gain a ζ-dependence, complicating the matter more. It will be interesting to study the full non-linear relation between the two, and use this for the inversion. We expect that when $\zeta \sim 1$, the non-linear effects will induce significant non-Gaussianity in the distribution for $\delta\rho$, even if ζ is Gaussian. A first study of these effects has been done recently in [42], and we hope to address them within our formalism.

Another assumption we made is that PBHs only form for spherically symmetric perturbations, allowing us to only consider spherical volumes. Although this is a reasonable approximation because PBHs are rare at formation and form from Hubble volumes which are spheres, it might be possible to take nonsphericity into account by defining the compaction function for general volumes and relating it to ζ. It is also unclear how this influences the criteria for PBH formation, so this might be an interesting line of numerical research.

A large reason why we introduced the Wigner function as probability distribution for the system in chapter 3 was that the state produced by inflation is Gaussian. While this has been confirmed by experiments, small non-Gaussianities might exist, and if they do they can play a large role. Even small deviations from Gaussian behaviour can have a large impact in the tail of a distribution, and because PBHs are rare they form precisely from this tail, so we would like to expand our theory to take small non-Gaussianities into account. This means that we have to include higher order terms in our density matrix, and that the Wigner function might lose its probabilistic interpretation. However, for small non-Gaussianities this should not be a big problem, especially if we assume no constraints on the momentum correlators and can integrate them out to get an always well-defined probability for ζ.

Finally, we would like to implement Musco's constraints more completely. We have argued why the $\partial_r \mathcal{C} = 0$ constraint will not alter the distribution very much, but we would still like to include it. One way this might be possible is to add terms of $e^{-(\partial_r \mathcal{C})^2/(2\sigma^2)}$ or $\theta(\partial_r \mathcal{C} + y) - \theta(\partial_r \mathcal{C} - y)$ to the path integral, with y and σ parametrizing how close to the radius a maximum has to be to count, but this is still work in progress. Also, we have not implemented the shape-dependence of $\mathcal{C}_c$ at all. The way this could be done is to let it be a functional of $\mathcal{C}$ in the path integral. The challenge of determining this form and solving the resultant path integral is also left for future work.

We have also seen that the momentum correlators are important for PBH formation, both potentially for the formation criterion and in the probability density for $\mathcal{C}$. Because PBHs cannot form from just slow roll inflation, we have no reason in general to expect them to be small. On the numerical side, to our knowledge it has not been studied how this influences formation and on the theoretical side, there is also not a lot known about what these correlators are like in theories of beyond slow roll inflation: this is an active research topic.

The calculations done in this thesis show that any amount of PBHs can be produced from inflation with an enhancement in the power spectrum on small scales, also precisely enough for them to be dark matter. This amount is however very sensitive to the size of the enhancement, and hence on the specific theory. Furthermore, since we know very light PBHs do not exist in large enough quantities, the physical PBH spectrum cannot be roughly scale invariant as it is in our model. Still, we have shown that the amount of PBHs in the universe is also a sensitive probe of the details of inflation, especially as any evidence of their existence will mean that the single field, slow roll picture is incomplete. Therefore, we hope that further study in this subject will allow us to shine more light on the mystery of what makes up the dark matter, what exactly happened during inflation, or both.

Chapter 6

Appendices

Appendix I

In this appendix, the following integral used in section 4.1 is solved:

$$I = \int_{-\infty}^{\infty} \frac{dx}{x - i\epsilon} e^{-ix\mathcal{C}_c - g(r)x^2} \tag{6.0.1}$$

We can do this by noting that it is the Fourier transform of a product of functions, and using that this is the convolution of the respective Fourier transforms this yields:

$$I = \mathcal{F}(\frac{1}{x - i\epsilon} e^{-g(r)x^2}; -\mathcal{C}_c) \tag{6.0.2}$$

$$= \mathcal{F}(\frac{1}{x - i\epsilon}) * \mathcal{F}(e^{-g(r)x^2}) \tag{6.0.3}$$

$$= \frac{1}{2\pi} \int_{-\infty}^{\infty} dy \mathcal{F}(\frac{1}{x - i\epsilon}; y - \mathcal{C}_c) \mathcal{F}(e^{-g(r)x^2}; -y). \tag{6.0.4}$$

The first Fourier transform is given by:

$$\mathcal{F}(\frac{1}{x - i\epsilon}; y - \mathcal{C}_c) = \int dx \frac{1}{x - i\epsilon} e^{ix(y - \mathcal{C}_c)}. \tag{6.0.5}$$

Here we note that the integrand goes to zero as $\mathrm{Im}(x)$ goes to ∞, so we can add a half- circular contour above the real axis and the integral over this will go to zero as the radius is taken to infinity and $y - \mathcal{C}_c > 0$. Then there is one pole at $x = i\epsilon$ inside the contour, which is a simple pole with residue 1. By the residue theorem we have that the integral yields $2\pi i$.

If $y - \mathcal{C}_c < 0$, a half-circular contour with radius tending to infinity can be added below the real axis, and then the integral over this will go to zero. As there are no

poles enclosed by this contour, by the residue theorem this integral yields zero, so we get:

$$\mathcal{F}(\frac{1}{x-i\epsilon};y-\mathcal{C}_c)=2\pi i\theta(y-\mathcal{C}_c). \tag{6.0.6}$$

Furthermore, by completing the square we have that:

$$\mathcal{F}(e^{-g(r)x^2};-y)=\int dxe^{-g(r)x^2-iyx}=\sqrt{\frac{\pi}{g(r)}}e^{-y^2/4g(r)}. \tag{6.0.7}$$

This yields:

$$I=\int_{-\infty}^{\infty}dyi\theta(\mathcal{C}_c-y)\sqrt{\frac{\pi}{g(r)}}e^{-y^2/4g(r)} \tag{6.0.8}$$

$$=i\int_{-\infty}^{\mathcal{C}_c}dy\sqrt{\frac{\pi}{g(r)}}e^{-y^2/4g(r)} \tag{6.0.9}$$

$$=i\pi\text{erfc}(\frac{\mathcal{C}}{2\sqrt{g(r)}}). \tag{6.0.10}$$

Appendix II

In this appendix, we show the calculation of the inverse kernel used in chapter 3. We prove that for:

$$K(q,q';t) = \frac{9}{32\pi^2}\int_0^\infty dk \frac{\mathcal{O}(k)}{k^4}\theta(k-q)\theta(k-q')q^2 q'^2. \tag{6.0.11}$$

Its inverse is given by:

$$K^{-1}(q,q') = -\int_0^\infty dk \frac{16\pi^2 k^4}{9\mathcal{O}(k)q^2 q'^2}\partial_q\delta(k-q)\partial_k\delta(k-q') + (q \leftrightarrow q'). \tag{6.0.12}$$

Using that K is symmetric, we have:

$$\int_0^\infty dk K(q,k)K^{-1}(k,q') = -\int_0^\infty dk dp dp' \frac{p'^4\mathcal{O}(p)}{p^4\mathcal{O}(p')}\frac{q^2}{q'^2}\theta(p-q)\theta(p-k)\partial_k\delta(p'-k)\partial_{p'}\delta(p'-q'). \tag{6.0.13}$$

After partial integration of the derivative on the first delta function this yields:

$$= -\int_0^\infty dk dp dp' \frac{p'^4\mathcal{O}(p)}{p^4\mathcal{O}(p')}\frac{q^2}{q'^2}\theta(p-q)\delta(p-k)\delta(p'-k)\partial_{p'}\delta(p'-q') \tag{6.0.14}$$

using that $\partial_k\theta(p-k) = -\delta(p-k)$. Now the integral over k can be done, yielding:

$$= -\int_0^\infty dp dp' \frac{p'^4\mathcal{O}(p)}{p^4\mathcal{O}(p')}\frac{q^2}{q'^2}\theta(p-q)\delta(p-p')\partial_{p'}\delta(p'-q'). \tag{6.0.15}$$

The integral over p can now be done using the delta function, which gives:

$$= -\int_0^\infty dp \frac{q^2}{q'^2}\theta(p-q)\partial_p\delta(p-q') \tag{6.0.16}$$

$$= \int_0^\infty dp \frac{q^2}{q'^2}\delta(p-q)\delta(p-q') \tag{6.0.17}$$

$$= \delta(q-q'). \tag{6.0.18}$$

Which is what we set out to prove.

Appendix III

In this appendix we derive the following results that are used in chapter 3:

$$\int_0^\infty dr \sin(kr)\sin(k'r) = \frac{\pi}{2}[\delta(k+k') - \delta(k-k')] \tag{6.0.19}$$

and

$$k' \int_0^\infty drr \sin(kr)\cos(k'r) = -\frac{\pi k'}{2}\frac{\partial}{\partial k}[\delta(k+k') + \delta(k-k')]. \tag{6.0.20}$$

At first, we have to note that these integrals clearly do not converge. However, we can regularize them by adding to the integrands a term of $e^{-\epsilon r}$ with $\epsilon > 0$ infinitesimal. This yields for the first integral:

$$\int_0^\infty dr \sin(kr)\sin(k'r)e^{-\epsilon r} = -\frac{1}{4}\int_0^\infty dr[e^{ikr} - e^{-ikr}][e^{ik'r} - e^{-ik'r}]e^{-\epsilon r} \tag{6.0.21}$$

$$= -\frac{1}{4}\int_0^\infty dr(e^{ir(k+k'+i\epsilon)} + e^{ir(-k-k'+i\epsilon)} - e^{ir(k-k'+i\epsilon)} - e^{ir(k'-k+i\epsilon)}) \tag{6.0.22}$$

$$= -\frac{1}{4}(\frac{e^{ir(k+k'+i\epsilon)}}{i(k+k'+i\epsilon)} + \frac{e^{ir(-k-k'+i\epsilon)}}{i(-k-k'+i\epsilon)} - \frac{e^{ir(k-k'+i\epsilon)}}{i(k-k'+i\epsilon)} - \frac{e^{ir(k'-k+i\epsilon)}}{i(k'-k+i\epsilon)})\Big|_{r=0}^{r=\infty} \tag{6.0.23}$$

$$= -\frac{i}{4}(\frac{1}{k+k'+i\epsilon} - \frac{1}{k+k'-i\epsilon} - \frac{1}{k-k'+i\epsilon} + \frac{1}{k-k'-i\epsilon}) \tag{6.0.24}$$

$$= -\frac{i}{4}(-\frac{2i\epsilon}{(k+k')^2+\epsilon^2} + \frac{2i\epsilon}{(k-k)'^2+\epsilon^2}). \tag{6.0.25}$$

The function $\frac{\epsilon}{\pi(x^2+\epsilon^2)}$ is also known as the Poisson kernel, and it reduces to the delta function in the limit when $\epsilon \to 0$. This means we have:

$$= \frac{1}{2}(\frac{\epsilon}{(k+k')^2+\epsilon^2} - \frac{\epsilon}{(k-k')^2+\epsilon^2}) \tag{6.0.26}$$

$$= \frac{\pi}{2}(\delta(k-k') - \delta(k-k')). \tag{6.0.27}$$

Now we derive the second integral, which goes similarly:

$$k' \int_0^\infty drr \sin(kr)\cos(k'r)e^{-\epsilon r} = \frac{k'}{4}\int_0^\infty drr[e^{ikr} - e^{-ikr}][e^{ik'r} + e^{-ik'r}]e^{-\epsilon r} \tag{6.0.28}$$

$$= \frac{k'}{4}\int_0^\infty dr r(e^{ir(k+k'+i\epsilon)} - e^{ir(-k-k'+i\epsilon)} + e^{ir(k-k'+i\epsilon)} - e^{ir(k'-k+i\epsilon)}) \tag{6.0.29}$$

$$= -\frac{k'}{4}\int_0^\infty dr(\frac{e^{ir(k+k'+i\epsilon)}}{i(k+k'+i\epsilon)} - \frac{e^{ir(-k-k'+i\epsilon)}}{i(-k-k'+i\epsilon)} + \frac{e^{ir(k-k'+i\epsilon)}}{i(k-k'+i\epsilon)} - \frac{e^{ir(k'-k+i\epsilon)}}{i(k'-k+i\epsilon)}) \tag{6.0.30}$$

$$= -\frac{k'}{4}(\frac{1}{(k+k'+i\epsilon)^2} - \frac{1}{(k+k'-i\epsilon)^2} + \frac{1}{(k-k'+i\epsilon)^2} - \frac{1}{(k-k'-i\epsilon)^2}) \tag{6.0.31}$$

$$= \frac{k'}{4}\frac{\partial}{\partial k}(\frac{1}{k+k'+i\epsilon} - \frac{1}{k+k'-i\epsilon} + \frac{1}{k-k'+i\epsilon} - \frac{1}{k'-k-i\epsilon}). \tag{6.0.32}$$

Using the same identities as before, this yields:

$$= -\frac{k'}{4}\frac{\partial}{\partial k}(\delta(k+k') + \delta(k-k')). \tag{6.0.33}$$

Appendix IV

In this appendix we derive the result for $\mathcal{O}$ in terms of the correlation functions used in section 3. We look at the density matrix for a Gaussian state, given by

$$\langle\phi|\rho(t)|\phi'\rangle = \mathcal{N}\exp\Big\{-\frac{1}{2}\int d\vec{x}d\vec{y}[\phi(\vec{x})A(\vec{x},\vec{y},t)\phi(\vec{y}) + \phi'(\vec{x})B(\vec{x},\vec{y},t)\phi'(\vec{y}) \tag{6.0.34}$$

$$- 2\phi(\vec{x})C(\vec{x},\vec{y},t)\phi'(\vec{y})]\Big\}. \tag{6.0.35}$$

We have from the paper by Koksma, Prokopec and Schmidt[40]:

$$\langle\hat{\phi}(\vec{x})\hat{\phi}(\vec{y})\rangle = F(\vec{x},\vec{y};t) = \frac{1}{2}\left(A_{\rm H} - C\right)^{-1}(\vec{x},\vec{y};t)' \tag{6.0.36}$$

$$\frac{1}{2}\langle\{\hat{\phi}(\vec{x}),\hat{\pi}(\vec{y})\}\rangle = \partial_{t'}F\left(\vec{x},t;\vec{y},t'\right)\big|_{t=t'} = \frac{1}{2}\,\mathrm{Tr}\left[\hat{\rho}_{\rm g}(t)\{\hat{\phi}(\vec{x}),\hat{\pi}(\vec{y})\}\right] \tag{6.0.37}$$

$$= -\frac{1}{2}\left(A_{\rm H} - C\right)^{-1}\cdot A_{\bar{\rm H}}(\vec{x},\vec{y};t) \tag{6.0.38}$$

$$\frac{1}{2}\langle\{\hat{\pi}(\vec{x}),\hat{\pi}(\vec{y})\}\rangle = \partial_t\partial_{t'}F\left(\vec{x},t;\vec{y},t'\right)\big|_{t=t'} = \frac{1}{2}\,\mathrm{Tr}\left[\hat{\rho}_{\rm g}(t)\{\hat{\pi}(\vec{x}),\hat{\pi}(\vec{y})\}\right] \tag{6.0.39}$$

$$= \frac{1}{2}\left[\frac{1}{2}A^\dagger\cdot\left(A_{\rm H} - C\right)^{-1}\cdot A + A\cdot\left(A_{\rm H} - C\right)^{-1}\cdot A^\dagger - C\cdot\left(A_{\rm H} - C\right)^{-1}\cdot C\right](\vec{x},\vec{y};t). \tag{6.0.40}$$

And we have the expression for $\mathcal{O}$ we need to determine:

$$\mathcal{O}(k,t) = \left(\mathcal{O}_1(k,t) - \frac{\mathcal{O}_3^2(k,t)}{4\mathcal{O}_2(k,t)}\right) \tag{6.0.41}$$

For which we have in real space:

$$\begin{aligned} 2\mathcal{O}_1 &= A + B + 2C - (A-B)\cdot(A+B-2C)^{-1}\cdot(A-B) \\ \mathcal{O}_2 &= 2(A+B-2C)^{-1} \\ \mathcal{O}_3 &= -i\left[(A-B)\cdot(A+B-2C)^{-1} + (A+B-2C)^{-1}\cdot(A-B)\right]. \end{aligned} \tag{6.0.42}$$

Because ρ is hermitian, we have $A^\dagger = B$ and $C^\dagger = C$. This means we have that $A + B = 2A_H$, and $A - B = 2iA_{\bar{H}}$, so these identities become:

$$\begin{aligned}\mathcal{O}_1 &= A_H + C + 2A_{\bar{H}} \cdot (2A_H - 2C)^{-1} \cdot A_{\bar{H}} \\ \mathcal{O}_2 &= 2(2A_H - 2C)^{-1} \\ \mathcal{O}_3 &= \left[A_{\bar{H}} \cdot (2A_H - 2C)^{-1} + (2A_H - 2C)^{-1} \cdot A_{\bar{H}}\right].\end{aligned} \tag{6.0.43}$$

From now on, we assume homogeneity and work in Fourier space, so the operators diagonalize and are all just k and time-dependent. We can then just divide and multiply their Fourier transforms. Doing this for the equations for the correlation functions we find that:

$$A_H - C = \frac{1}{2\langle\zeta\zeta^*\rangle} \tag{6.0.44}$$

and

$$A_{\bar{H}} = -\frac{\langle\zeta\pi^* + \pi\zeta^*\rangle}{2\langle\zeta\zeta\rangle}. \tag{6.0.45}$$

Then in terms of these, the operators become:

$$\mathcal{O}_1 = (A_H + C) + \frac{\langle\zeta\pi^* + \pi\zeta^*\rangle^2}{2\langle\zeta\zeta\rangle} \tag{6.0.46}$$

$$\mathcal{O}_2 = 2\langle\zeta\zeta^*\rangle \tag{6.0.47}$$

$$\mathcal{O}_3 = -2\langle\zeta\pi^* + \pi\zeta^*\rangle. \tag{6.0.48}$$

Filling this into equation 5.3.10 yields:

$$\mathcal{O} = (A_H + C) = \frac{1}{2\langle\zeta\zeta^*\rangle}\frac{A_H + C}{A_H - C}. \tag{6.0.49}$$

This fraction is exactly the Gaussian invariant Δ^2, which is defined in real space in [40] as:

$$\Delta^2(\vec{x}, \vec{y}; t) = \langle\zeta(\vec{x})\zeta(\vec{y})\rangle\langle\Pi(\vec{x})\Pi(\vec{y})\rangle - \frac{1}{4}\langle\{\zeta(\vec{x}), \Pi(\vec{y})\}\rangle^2, \tag{6.0.50}$$

where all the correlators are taken at equal time t. Therefore, we find the following for $\mathcal{O}$:

$$\mathcal{O}(k, t) = \frac{\Delta^2(\vec{k}, t)}{2\langle\zeta(\vec{k}, t)\zeta^*(\vec{k}, t)\rangle}. \tag{6.0.51}$$

Bibliography

[1] G. Bertone and D. Hooper, "History of dark matter," Rev. Mod. Phys. **90** (2018) no.4, 045002 doi:10.1103/RevModPhys.90.045002.

[2] B. Carr, F. Kuhnel and M. Sandstad, Phys. Rev. D **94** (2016) no.8, 083504 doi:10.1103/PhysRevD.94.083504.

[3] S. Hawking, "Gravitationally collapsed objects of very low mass," Mon. Not. Roy. Astron. Soc. **152** (1971) 75.

[4] Ya. B. Zel'dovich and I. D. Novikov "The Hypothesis of Cores Retarded during Expansion and the Hot Cosmological Model" Soviet Astronomy, Vol. 10 (1967), p.602

[5] I. Musco, "The threshold for primordial black holes: dependence on the shape of the cosmological perturbations," arXiv:1809.02127 [gr-qc].

[6] J. R. Oppenheimer and G. M. Volkoff, "On Massive neutron cores," Phys. Rev. **55** (1939) 374.

[7] F. Zwicky, "Die Rotverschiebung von extragalaktischen Nebeln," Helv. Phys. Acta **6** (1933) 110 [Gen. Rel. Grav. **41** (2009) 207].

[8] F. Zwicky, "On the Masses of Nebulae and of Clusters of Nebulae," Astrophys. J. **86** (1937) 217.

[9] D. H. Rogstad and G. S. Shostak, " Gross Properties of Five Scd Galaxies as Determined from 21-CENTIMETER Observations," Astrophysical Journal, vol. 176 (1972), p.315 doi: 10.1086/151636

[10] S. M. Carroll, "Spacetime and geometry: An introduction to general relativity," San Francisco, USA: Addison-Wesley (2004) 513 p.

[11] N. Aghanim *et al.* [Planck Collaboration], "Planck 2018 results. VI. Cosmological parameters," arXiv:1807.06209 [astro-ph.CO].

[12] H. Reeves, J. Andouze, W. A. Fowler and D. N. Schramm, "On The Origin Of Light Elements," Astrophys. J. **179** (1973) 909.

[13] E. Aprile *et al.* [XENON Collaboration], "Constraining the spin-dependent WIMP-nucleon cross sections with XENON1T," Phys. Rev. Lett. **122** (2019) no.14, 141301 doi:10.1103/PhysRevLett.122.141301.

[14] H. Baer, V. Barger, S. Salam, H. Serce and K. Sinha, "LHC SUSY and WIMP dark matter searches confront the string theory landscape," JHEP **1904** (2019) 043 doi:10.1007/JHEP04(2019)043

[15] L. D. Duffy and K. van Bibber, "Axions as Dark Matter Particles," New J. Phys. **11** (2009) 105008.

[16] D. Clowe, M. Bradac, A. H. Gonzalez, M. Markevitch, S. W. Randall, C. Jones and D. Zaritsky, "A direct empirical proof of the existence of dark matter," Astrophys. J. **648** (2006) L109

[17] Carr, B. J., "The primordial black hole mass spectrum" 1975 ,Astrophysical Journal, vol. 201,(1975), pt. 1, p. 1-19.

[18] B. J. Carr and S. W. Hawking, "Black holes in the early Universe," Mon. Not. Roy. Astron. Soc. **168** (1974) 399.

[19] C. Alcock *et al.* [MACHO Collaboration], "The MACHO project: Microlensing results from 5.7 years of LMC observations," Astrophys. J. **542** (2000) 281

[20] B. Carr, "Primordial black holes as dark matter and generators of cosmic structure," arXiv:1901.07803 [astro-ph.CO].

[21] D. Baumann, "TASI lectures on Inflation," doi:10.1142/97898143271830010 arXiv:0907.5424 [hep-th].

[22] C. Germani and I. Musco, "Abundance of Primordial Black Holes Depends on the Shape of the Inflationary Power Spectrum," Phys. Rev. Lett. **122** (2019) no.14, 141302 doi:10.1103/PhysRevLett.122.141302.

[23] J. M. Ezquiaga and J. García-Bellido, "Quantum diffusion beyond slow-roll: implications for primordial black-hole production," JCAP **1808** (2018) 018.

[24] A. M. Green and A. R. Liddle, "Constraints on the density perturbation spectrum from primordial black holes," Phys. Rev. D **56** (1997) 6166.

[25] A. M. Green, A. R. Liddle, K. A. Malik and M. Sasaki, "A New calculation of the mass fraction of primordial black holes," Phys. Rev. D **70** (2004) 041502.

[26] C. Germani and T. Prokopec, "On primordial black holes from an inflection point," Phys. Dark Univ. **18** (2017) 6 doi:10.1016/j.dark.2017.09.001

[27] C. Pattison, V. Vennin, H. Assadullahi and D. Wands, "Quantum diffusion during inflation and primordial black holes," JCAP **1710** (2017) no.10, 046.

[28] A. A. Starobinsky, "A New Type of Isotropic Cosmological Models Without Singularity," Phys. Lett. B **91** (1980) 99.

[29] A. H. Guth, "The Inflationary Universe: A Possible Solution to the Horizon and Flatness Problems," Phys. Rev. D **23** (1981) 347.

[30] A. D. Linde, "A New Inflationary Universe Scenario: A Possible Solution of the Horizon, Flatness, Homogeneity, Isotropy and Primordial Monopole Problems," Phys. Lett. **108B** (1982) 389

[31] J. M. Maldacena, "Non-Gaussian features of primordial fluctuations in single field inflationary models," JHEP **0305** (2003) 013 doi:10.1088/1126-6708/2003/05/013 [astro-ph/0210603].

[32] T. Prokopec, Lecture notes on Cosmology for the course NS-TP430M (2014).

[33] R. L. Arnowitt, S. Deser and C. W. Misner, "Dynamical Structure and Definition of Energy in General Relativity," Phys. Rev. **116** (1959) 1322.

[34] V. F. Mukhanov, H. A. Feldman and R. H. Brandenberger, "Theory of cosmological perturbations. Part 1. Classical perturbations. Part 2. Quantum theory of perturbations. Part 3. Extensions," Phys. Rept. **215** (1992) 203. doi:10.1016/0370-1573(92)90044-Z

[35] J. M. Bardeen, P. J. Steinhardt and M. S. Turner, "Spontaneous Creation of Almost Scale - Free Density Perturbations in an Inflationary Universe," Phys. Rev. D **28** (1983) 679.

[36] Y. B. Zeldovich, "A Hypothesis, unifying the structure and the entropy of the universe," Mon. Not. Roy. Astron. Soc. **160** (1972) 1P.

[37] J. Garcia-Bellido and E. Ruiz Morales, "Primordial black holes from single field models of inflation," Phys. Dark Univ. **18** (2017) 47 doi:10.1016/j.dark.2017.09.007

[38] J. M. Ezquiaga, J. Garcia-Bellido and E. Ruiz Morales, "Primordial Black Hole production in Critical Higgs Inflation," Phys. Lett. B **776** (2018) 345.

[39] J. F. Koksma, T. Prokopec and G. I. Rigopoulos, Class. Quant. Grav. **25** (2008) 125009 doi:10.1088/0264-9381/25/12/125009.

[40] J. F. Koksma, T. Prokopec and M. G. Schmidt, "Entropy and Correlators in Quantum Field Theory," Annals Phys. **325** (2010) 1277 doi:10.1016/j.aop.2010.02.016.

[41] P. Friedrich, M. Gambino and T. Prokopec, in progress.

[42] S. Young, I. Musco and C. T. Byrnes, "Primordial black hole formation and abundance: contribution from the non-linear relation between the density and curvature perturbation," arXiv:1904.00984 [astro-ph.CO].